INTERNATIONAL ATOMIC ENERGY AGENCY
UNITED NATIONS EDUCATIONAL, SCIENTIFIC AND CULTURAL ORGANIZATION

INTERNATIONAL CENTRE FOR THEORETICAL PHYSICS
34100 TRIESTE (ITALY) - P.O.B. 586 - MIRAMARE - STRADA COSTIERA 11 - TELEPHONE: 2240-1
CABLE: CENTRATOM - TELEX 460392 - I

SMR/406-8

THIRD AUTUMN WORKSHOP ON ATMOSPHERIC RADIATION AND CLOUD PHYSICS
27 November - 15 December 1989

"Radiation and Energy Tranport in the Earth Atmospheric System"

Hans-Juergen BOLLE
Institut für Meteorologie/
Atmosphärische Wissenschaften
Fachrichtung Klima
Freie Universität Berlin
Berlin
Federal Republic of Germany

The basic quantitity to describe the spatial distribution of radiant power in an electromagnetic radiation field is the radiant power area-density per unit solid angle. It is specified as the flux Φ of radiant energy (Q) per unit time across unit area into a cone defined by the unit solid angle, and is called *radiance* with the symbol L. If the radiation field is inhomogenous it is preferable to define the radiance for increments of the area (dA) and of the solid angle ($d\Omega$), and to take into account the angle ϑ between the direction of the electromagnetic wave and the normal of the incremental area dA (compare Fig. 2). The projection of dA in the

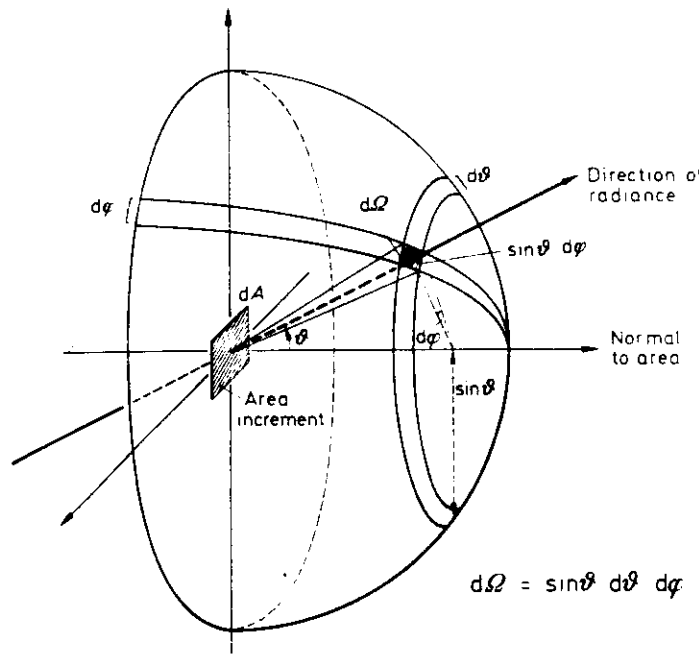

Fig. 2. Radiance geometry and definition of solid angle

direction $d\Omega$ is $\cos\vartheta\, dA$ and

$$L = \frac{d^2\Phi}{\cos\vartheta\, dA\, d\Omega}. \tag{3}$$

The radiance L is measured in $W\,m^{-2}\,sr^{-1}$.

The radiant flux incident onto unit area from all directions of the hemisphere is called *irradiance* E. Its unit is $W\,m^{-2}$. It can be derived from the radiance by integrating over the hemisphere $2\pi\Omega_0$, Ω_0 = unit solid angle,

$$E = \frac{d\Phi}{dA} = \int_0^{2\pi\Omega_0} L\cos\vartheta\, d\Omega\ W\,m^{-2}. \tag{4}$$

The *radiant energy* transported across a defined area during the time t' is measured in W s or Joule (J) and is given by

$$Q = \int_0^{t'} \Phi\, dt. \tag{5}$$

The energy received during a time interval t_1, t_2 at unit area is called the *radiant exposure* H,

$$H = \int_{t_1}^{t_2} E\, dt, \tag{6}$$

and is measured in $J\,m^{-2}$ per specified exposure time.

Only for point sources the expression

$$I = \mathrm{d}\Phi/\mathrm{d}\Omega \tag{7}$$

may be used. It is called *intensity* and is measured in $\mathrm{W\,sr^{-1}}$.

If one considers an extended radiation source its radiant power per unit area is expressed by the *radiant exitance* M, which has the same dimension as the irradiance, $\mathrm{W\,m^{-2}}$. The total flux from the source is determined by integration over the surface A of the source:

$$\Phi = \int_A M \,\mathrm{d}A\,. \tag{8}$$

If the source is a *black body* – defined as an enclosed volume which is in thermodynamic equilibrium at constant temperature – the exitance is conveniently distinguished by an index B:

$$M_B = \text{exitance of a black body}\,. \tag{9}$$

In practise a black body is constructed as a box with its skin kept at constant temperature. A hole much smaller than the surface of the box serves as emitting area. The radiance resulting from such a source is related to its exitance by (compare Fig. 2)

$$M_B = \int_0^{2\pi\Omega_0} L_{B,\perp} \cos\vartheta \,\mathrm{d}\Omega = 2\pi \int_0^{\pi/2} L_{B,\perp} \sin\vartheta\cos\vartheta \,\mathrm{d}\vartheta\,, \tag{10}$$

where $L_{B,\perp}$ is the black body radiance normal to the radiating aperture and $\cos\vartheta$ arises from the orientation of the incremental cone $\mathrm{d}\Omega$ with respect to the normal of the emitting area. For the radiance emerging normally from the black body opening, $L_{B,\perp}$, the symbol $B(T)$ is introduced. This quantity depends solely on the black body temperature. The integration of Eq. (10) then results in

$$M_B = \pi B(T) \equiv \pi L_{B,\perp}\,. \tag{11}$$

The radiant energy traversing unit area per unit time, the *radiant flux* (surface) *density* is denoted by either M or E.

Spectral radiation quantities are obtained by differentiation of the quantities defined in Eqs. (3) through (11) to one of the spectral parameters: *frequency* (f or ν), *wavelength* (λ) or *wavenumber* ($\bar{\nu}$). The use of the wavenumber is very convenient for spectroscopic considerations. It is defined by

$$\bar{\nu} = 1/\lambda \tag{12}$$

and is measured in $\mathrm{cm^{-1}}$. The spectral radiance can e.g. be expressed by

$$L_\lambda = \frac{dL}{\mathrm{d}\lambda} = \frac{\mathrm{d}^3\Phi}{\cos\vartheta\,\mathrm{d}A\,\mathrm{d}\Omega\,\mathrm{d}\lambda}\ \mathrm{W\,m^{-2}\,sr^{-1}\,nm^{-1}} \tag{13}$$

if the wavelength is measured in nm, or by

$$L_{\bar{\nu}} = \frac{\mathrm{d}L}{\mathrm{d}\bar{\nu}} = \frac{\mathrm{d}^3\Phi}{\cos\vartheta\,\mathrm{d}A\,\mathrm{d}\Omega\,\mathrm{d}\bar{\nu}}\ \mathrm{W\,m^{-2}\,sr^{-1}(cm^{-1})^{-1}} \tag{14}$$

if the wavenumber (in $\mathrm{cm^{-1}}$) is used.

It should be noted here that the energy in a certain spectral band $\lambda_1 \ldots \lambda_2$ must be the same whether λ or $\tilde{\nu}$ is used:

$$\int_{\lambda_1}^{\lambda_2} L_\lambda \mathrm{d}\lambda = \int_{\tilde{\nu}_1 = \frac{1}{\lambda_1}}^{\tilde{\nu}_2 = \frac{1}{\lambda_2}} L_{\tilde{\nu}} \mathrm{d}\tilde{\nu}. \tag{15}$$

Therefore the relation holds

$$L_\lambda \mathrm{d}\lambda = L_{\tilde{\nu}} \mathrm{d}\tilde{\nu} \tag{16}$$

or

$$L_{\tilde{\nu}} = L_\lambda \frac{\mathrm{d}\lambda}{\mathrm{d}\tilde{\nu}} = \lambda^2 L_\lambda = \tilde{\nu}^{-2} L_\lambda. \tag{17}$$

Spectral distributions look therefore quite different if the wavelength or the wavenumber is used as independent variable.

The loss of electromagnetic energy out of a beam either by a change in direction due to scattering or by absorption can be described by Beer's law which states that the loss is proportional to the incident energy:

$$\mathrm{d}L = -\sigma_e L \,\mathrm{d}s = -L \,\mathrm{d}u\,, \tag{18}$$

where $\mathrm{d}u = \sigma_e \,\mathrm{d}s$ is the differential of the *optical path length*[3], $\mathrm{d}s$ is the incremental *geometrical path length*, and σ_e is the *linear extinction* or *attenuation coefficient* with the dimension m^{-1}. Alternatively the attenuation can be described by

$$\mathrm{d}L = -\sigma_{e,m} L \mathrm{d}m = -L \,\mathrm{d}u\,, \tag{19}$$

where $\mathrm{d}m = \varrho \,\mathrm{d}s$ is the *mass surface density* and $\sigma_{e,m}$ the *mass extinction coefficient* measured in $\mathrm{kg}^{-1}\,\mathrm{m}^2$ (or $\mathrm{molecules}^{-1}\,\mathrm{m}^2$).

For pure scattering and pure absorption separate attenuation coefficients are introduced: the *scattering coefficient* σ (respectively σ_m) and the *absorption coefficient* a (respectively a_m). If both attenuation processes occur in the same path, the total attenuation coefficient will be

$$\sigma_e = \sigma + a\,, \tag{20}$$

and if different (N) substances are involved it is convenient to write

$$\mathrm{d}u = \sum_{i=1}^{N} (\sigma_{m,i} + a_{m,i})\, \varrho_i \mathrm{d}s\,. \tag{21}$$

The *reflection* by the atmosphere including its aerosols and clouds is essentially a *backward scattering* process. This is also true for natural earth surfaces where

3 In the U.I.P. Document 20 (1978) on Symbols, Units, and Nomenclature in Physics the symbol μ is prescribed for the attenuation coefficient, and the Radiation Commission of the International Association for Meteorology and Atmospheric Physics (1978) has proposed δ for the optical path length (thickness). Since μ is widely used for the cosine of the zenith angle or the scattering angle in atmospheric radiative transfer theory, the symbol σ is used here for attenuation by scattering and σ_e for the total attenuation (extinction). Other authors prefer the symbols β or K instead of σ_e. For the optical path length the symbol u will be used here because δ may be confused with mathematical symbols. δ will exclusively be used here for the optical depth of the atmosphere, that is the optical path for a photon travelling vertically through the atmosphere. Other proposals for symbols made by the Radiation Commission are slightly adjusted in order to eliminate conflicts with the U.I.P. (1978) document

the electromagnetic waves are scattered at soil grains, cell structures in plant leaves or capillary waves on water surfaces. The radiation reflected from natural objects will therefore almost always be a mixture of a specular component and a diffuse component. Some objects like grass may come very close to a completely diffuse reflector, while quiet water surfaces are almost reflecting like a mirror. In many cases the *reflection function* (reflected radiance versus direction) can only be obtained empirically. The different reflection geometries are distinguished by the distribution of the incoming and the outgoing radiation. The quantities used for the description of the reflection properties are listed in Table 1. The symbols Ω_i, Ω_r stand for the solid angles of the incoming, respectively the outgoing radiation.

The transmitted radiation needs an analogue treatment as presented for the reflectance in Table 1.

If *spectral material properties* are considered this has to be expressed in terms of a functional dependence like

$$\begin{aligned} a(\lambda) &= (\Phi_{a\lambda}/\Phi_{0\lambda})_\lambda \quad \text{spectral absorptance} \\ \varrho(\lambda) &= (\Phi_{\varrho\lambda}/\Phi_{0\lambda})_\lambda \quad \text{spectral reflectance} \\ \tau(\lambda) &= (\Phi_{\tau\lambda}/\Phi_{0\lambda})_\lambda \quad \text{spectral transmittance}, \end{aligned} \tag{22}$$

where Φ_a, Φ_ϱ, Φ_τ and Φ_0 are the absorbed, reflected, transmitted and incident fluxes respectively, and $\Phi_\lambda = \mathrm{d}\Phi(\lambda)/\mathrm{d}\lambda$.

The *spectrum* which is of interest for energy processes in the earth-atmosphere system can roughly be divided into the following intervals:

$\lambda(\mu m)$	$\bar{\nu}(cm^{-1})$	Notation
$< 10^{-6}$	$> 10^{10}$	γ-ray radiation
$10^{-6} - 10^{-2}$	$10^{6} - 10^{10}$	X-ray radiation
0.01– 0.38	26.316 – 10^{6}	ultraviolett radiation
0.38– 0.78	12.820 – 26.316	visible light
0.78– 2.5	4.000 – 12.820	solar infrared radiation
2.5 – 1,000	0.1– 4.000	terrestrial infrared radiation
> 1,000	< 0.1	microwave radiation

The spectrum which is of interest for atmospheric research extends over the wide range from about 1 nm to 1 m wavelength as demonstrated in Fig. 3. For the energy processes in the lower atmosphere and at the ground only a small fraction of this spectrum is important. 98% of the energy reaching the earth from the sun is concentrated between 0.3 and 4 μm and 98% of the longwave radiation emitted from the earth to space is concentrated between 5 and 60 μm. Only about 2 octaves of the whole spectrum are responsible for the temperature distribution and biological processes on earth. Shorter wavelengths have special importance for the photo-chemistry in the upper atmosphere because of their high photon energy. Long wavelengths are of interest for radio communication and remote sensing of the earth.

As indicated in Fig. 3 there are different nomenclatures in use for the infrared part of the spectrum. For a description of the energetics of the earth-atmosphere system it is appropriate to discriminate between infrared energy from the sun up

Table 1. Nomenclature for reflection quantities

Incoming radiation	Outgoing radiation	Terminus	Symbol and definition	Unit
Directional	Directional	Reflection function	$\gamma_r(\Omega_i, \Omega_r) = \frac{d^3\Phi_r(\Omega_i, \Omega_r)}{\cos\vartheta_r \cdot d\Omega_r \cdot \cos\vartheta_i dE_i(\Omega_i) dA}$	sr^{-1}
Directional	Directonal	Reflection indicatrix	$\xi_r(\Omega_i, \Omega_r) = \pi\Omega_0\gamma_r(\Omega_i, \Omega_r)/\varrho(\Omega_i)$	
Directional	Hemispherical	Hemispherical reflectance for directional incidence	$\varrho(\Omega_i) = \int_{2\pi} \gamma_r(\Omega_i, \Omega_r)\cos\vartheta_r d\Omega_r$	
Hemispherical	Directional	Reflection source function	$J_r(\Omega_r) = \int_{2\pi} \gamma_r(\Omega_i, \Omega_r)\cos\vartheta_i dE_i(\Omega_i)$	$Wm^{-2}sr^{-1}$
Hemispherical	Directional	Directional reflectance factor for hemispherical incidence	$\varrho(\Omega_r) = \frac{J_r(\Omega_r) \cdot \pi\Omega_0}{E_i}$	
Hemispherical	Hemispherical	Albedo (reflectance)	$\varrho = \Phi_r/\Phi_i$	
			$E_i = \int_{2\pi} \cos\vartheta_i dE_i(\Omega)\ W \cdot m^{-2}$	

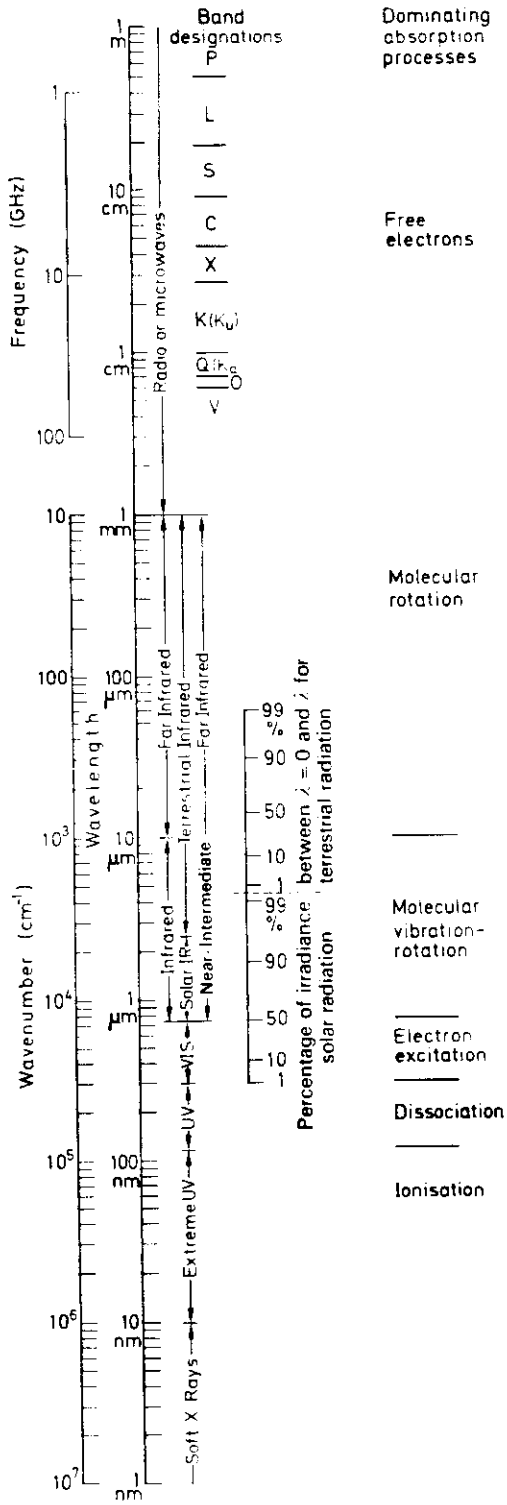

Fig. 3. Electromagnetic spectrum of the sun and terrestrial sources

to wavelengths of 2.5 μm (compare e.g. Fig. 14), and the emission of terrestrial sources which just starts to dominate the radiation field beyond 2.5 μm.

A compilation of the symbols used for the different quantities as well as of numerical values and units is given in the Appendix.

Emission Under Thermodynamic Equilibrium Conditions

According to Kirchhoff's Law the emission from a body equals the radiant exitance of a black body times the absorption coefficient of the (non black) material:

$$M = a M_B(T). \tag{85}$$

According to Planck the spectral black body exitance, its non-polarized emission from an unit area into the hemisphere, is a function of the temperature only, and is represented in dependence of the wavelength by the expression.

$$M_{B,\lambda}(T) = c_1 \lambda^{-5} (e^{c_2/\lambda T} - 1)^{-1} \tag{86}$$

and in dependence of the wavenumber by

$$M_{B,\bar{\nu}}(T) = c_1 \bar{\nu}^3 (e^{c_2 \bar{\nu}/T} - 1)^{-1} \tag{87}$$

with $c_1 = 2\pi hc^2 = 3.7418 \cdot 10^{-16}$ W m^{-2} first radiation constant
$c_2 = hc/k = 1.4388 \cdot 10^{-2}$ m K second radiation constant
$h = 6.6262 \cdot 10^{-34}$ J s Planck constant
$k = 1.3807 \cdot 10^{-23}$ J K^{-1} Boltzman constant
$c = 2.9979 \cdot 10^{8}$ m s^{-1} speed of light in vacuum.

Figure 8 gives the exitance for the wavelength range 1–100 μm and the temperature range 50–6,000 K. Accordingly the spectral radiance $L_{B,\bar{\nu}}$ of a black body normal to the radiating unit area, for which the symbol $B_{\bar{\nu}}(T)$ will be used, is

$$B_{\bar{\nu}}(T) = M_{B,\bar{\nu}}(T)/\pi. \tag{88}$$

Its unit is W m^{-2}sr^{-1} (cm^{-1})$^{-1}$ respectively W m^{-2}sr^{-1} μm^{-1} if the quantity $B_\lambda(T)$ is used.

In the atmosphere the basic proposition for black body emission, the thermodynamic equilibrium, is, strictly speaking, not completely achieved. Photons emitted at one altitude of the atmosphere will interact with molecules at another altitude where the population of the different involved rotational energy levels may be slightly different, because of a difference in the temperature due to the vertical atmospheric temperature gradient. For the atmosphere the expression "*local thermodynamic equilibrium*" (LTE) is commonly used if one refers to a situation where deviations from the thermodynamic equilibrium are negligible. At lower pressures the transfer of absorbed radiant energy into translational energy due to collisions takes longer because the mean free path length of a molecule increases. Careful studies of this problem have resulted in the conclusion that deviations from LTE can be neglected in most cases up to altitudes of ~ 70 km but become essential for the thermosphere [39].

For a horizontally infinite column of atmospheric gases the exitance can be derived in the following way. An infinitesimal path ds' in the column emits proportional to the radiating mass $\varrho(s')\,ds'$ [$\varrho(s')$ is the mass area density measured in kg m^{-2}], and a so far unknown source function $X_{\bar{\nu}}(T)$. The spectral radiance emerging from ds' around s' can be written (Fig. 9):

$$dL_{\bar{\nu}}(s') = \varrho(s') X_{\bar{\nu}}[T(s')]\, ds'. \tag{89}$$

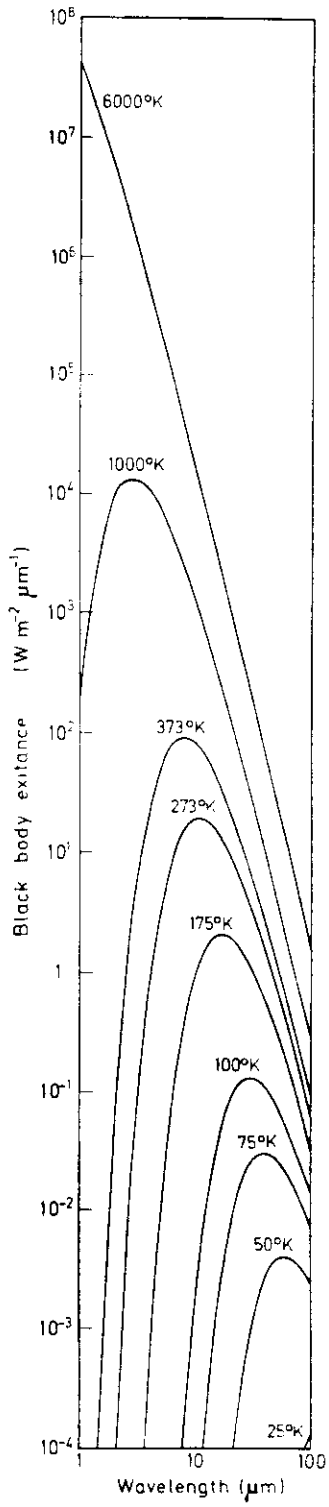

Fig. 8. Black body exitance. Emission of black body into the hemisphere for temperatures between 50 and 6,000 K and 1–100 nm wavelength

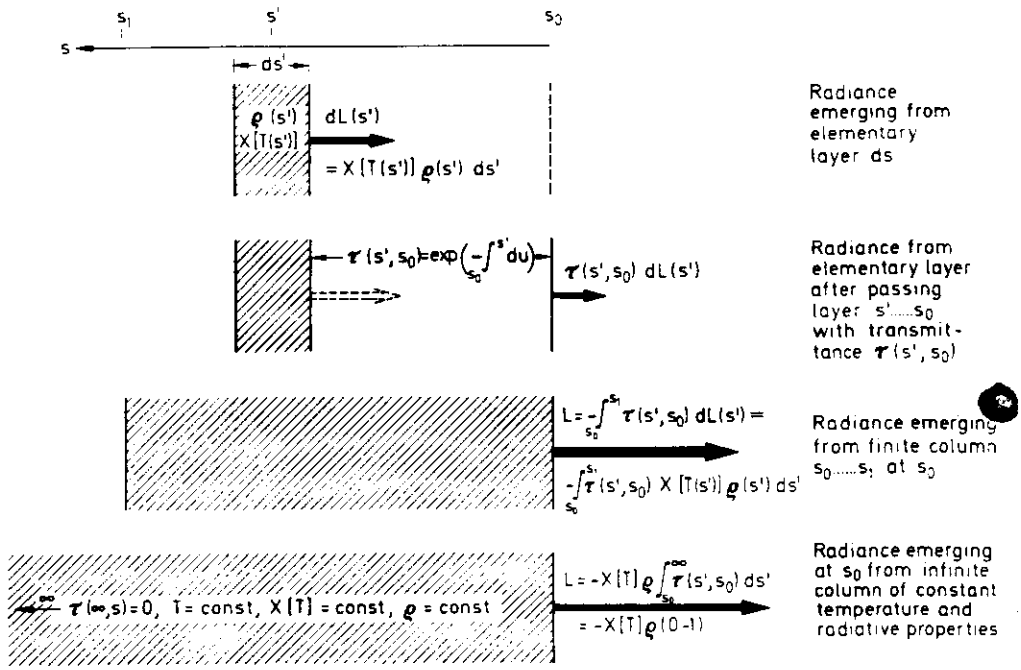

Fig. 9. Derivation of column radiance, Eq. (92)

At an observer posted at s_0 arrives only a fraction of the radiation emitted at s' because of the absorption between s' and s_0. According to Beer's law this fraction is given by the transmission function:

$$\tau(\bar{\nu}; s', s_0) = \exp\left\{-\int_{s_0}^{s'} a_m(\bar{\nu}; s)\,\varrho(s)\,\mathrm{d}s\right\}. \tag{90}$$

The integral in the r.h.s. exponential function is the (spectral) *optical path length* u_ν:

$$u(\bar{\nu}; s', s_0) = \int_{s_0}^{s'} a_m(\bar{\nu}; s)\varrho(s)\,\mathrm{d}s. \tag{91}$$

The absorption coefficient a_m is here defined per mass area density (mass absorption coefficient).

From an air column between $u(s_1)$ and $u(s_0=0)$ the following radiance is emerging (for the moment the spectral index $\bar{\nu}$ will be dropped):

$$\begin{aligned} L(s_1, s_0) &= -\int_0^{s_1} \tau(s', s_0)\,\mathrm{d}L(s') \\ &= -\int_0^{s_1} \varrho(s')\,X[T(s')]\,\mathrm{e}^{-\int_0^{s'} \varrho(s) a_m(s)\,\mathrm{d}s}\,\mathrm{d}s' \\ &= -\int_0^{s_1} \frac{X[T(s')]}{a_m(s')}\left(\frac{\mathrm{d}\tau(s', s_0)}{\mathrm{d}s'}\right)\mathrm{d}s \\ &= -\int_1^{\tau(s_1, s_0)} \frac{X[T(s)]}{a_m(s)}\,\mathrm{d}\tau. \end{aligned} \tag{92}$$

If we now assume that the air column is enclosed in a black body of constant temperature T of semi-infinite extension, the expression (92) must equal the radiance of a black body at temperature T for $\tau(s_1, s_0) \to 0$:

$$L(s_1 \to \infty, s_0 = 0) = L_{\mathrm{Bl}}(T) = B(T). \tag{93}$$

For T=constant and $a_m(s)$=constant Eq. (92) can be integrated between $s_0=0$ and $s=\infty$ with $\tau(\infty, 0)=0$ and $\tau(0, 0)=1$ and it results

$$B(T)=-\int_1^0 \frac{X(T)}{a_m}\mathrm{d}\tau=\frac{X(T)}{a_m} \tag{94}$$

or

$$X_\nu(T)=a_m(\tilde{\nu})\,B_\nu(T)\,. \tag{95}$$

With Eq. (95) the general result has been obtained that in a gasous medium the source function for the radiance $L=M\,\pi$ is equal to the Planck function times the absorption coefficient as long as LTE can be presumed.

Non-Thermal Emissions in the Upper Atmosphere

At reduced pressures with increased free path lengths the quenching of excited states due to collisions is reduced. The times between collisions (10^{-10} s at the surface, 10^{-5} s and 10^{-4} s in 75 km resp. 90 km altitude) may become longer than the life time of excited molecules and atoms. In this case the molecule or atom will emit one or more photons to get back into its ground level. In the course of this process even transitions may occur which under other circumstances are forbidden by quantum theory.

Often the excited species are dissociation products. Table 5 compiles the most prominent emissions which are observed as airglow [57–60]. Other emissions which are correlated to the intensity of the atomic oxygen green line (557.7 nm) are from molecular oxygen and include the Herzberg bands in the near ultraviolett and in the blue part of the spectrum, the Chamberlain bands in the blue, a continuum in the green and an emission at 864.5 nm which belongs to the "atmospheric" band system (Kaplan-Meinel bands). The total emission of these bands is about 3 kR. Rayleigh (R) is an often used unit for the rate of photon emission per unit area in a column ($s^{-1}\,m^{-2}$). For conversion into SI Units see Table 5. The conversion becomes difficult in case of structured broad band features. The emission orginates around 100 km altitude.

The "normal" airglow emission is strongly enhanced at high latitudes during solar activity which generates the aurora. Other emissions partly from highly excited atoms are at that time observed in addition. These emissions are excited by high energy electrons and protons which are emitted by the sun during eruptions or captured in the Van Allan belts of the earth from where they are discharged into the atmosphere.

Atmospheric Radiation Field

Solar Radiation

Extraterrestrial Solar Spectrum

The problem to measure the extraterrestrial solar spectrum and its possible variations is not yet solved satisfactorily. The corrections which have to be applied to ground based measurements due to the atmospheric extinction in the ultraviolett

Table 5. Prominent non-thermal atmospheric emissions and the OI far infrared emission ($I\,R \cong 1.58\,\lambda^{-1} \cdot 10^{-16}\,Wm^{-2}sr^{-1}$, λ in m)

Specie	Transition	Wavelength μm	Height range km	Intensity (kR)		Approx. radiance $Wm^{-2}\,sr^{-1}$	Producing	
				Day	Night		Reaction	Wavelength (nm)
N	$2p^2D \rightarrow 2p^2S$	0.5199	150–280	0.05			$N_2 + e^- \rightarrow N + N(^2D) + e$ $N_2 + h\nu \rightarrow N + N(^2D)$ $NO^+ + e \rightarrow N(^2D) + O$ u. a.	80–100
O	$^1S \rightarrow {}^1D$	0.5577	90–220	3	0.25	$0.7 \cdot 8.5 \cdot 10^{-7}$	$O + O + O \rightarrow O_2 + O(^1S)$	<242 <313 313–350
O	$^1D_2 \rightarrow {}^3P_2$ $^1D_2 \rightarrow {}^3P_1$	0.6300 0.6364	100–400	2–20	< 0.5	$1.3 \cdot 50 \cdot 10^{-7}$	$O_2 + h\nu \rightarrow O(^1D) + O(^3P)$ $O_3 + h\nu \rightarrow O(^1D) + O_2(^1\Delta_g)$	
O_2	$b^1\Sigma_g^+ \rightarrow X^3\Sigma_g^+$	0.7619(0–0) 0.8645(0–1)	< 50–100	300	6	$0.12 \cdot 6 \cdot 10^{-5}$	$O_3 + h\nu \rightarrow O_2(b^1\Sigma_g^+) + O(^3P)$	
Na	$3p^2P^0_{\frac{1}{2},\frac{3}{2}} \rightarrow 3s^2S_{\frac{1}{2}}$	0.5890 0.5896	70–110	0.1–0.3			$NaO + O \rightarrow Na(^2P) + O_2$ $NaH + O \rightarrow Na(^2P) + OH$ $NaH + H \rightarrow Na(^2P) + H_2$	
O_2	$a^1\Delta_g \rightarrow X^3\Sigma_g^-$	1.270(0–0) 1.58(0–1)	40–85	$2 \cdot 10^4$	80	$0.096\text{–}25 \cdot 10^{-4}$	$O_3 + h\nu \rightarrow O(^3P) + O_2(a^1\Delta_g)$	
OH	Vibr. bands $v \leq 9$	0.382–4.500	55–95	$3 \cdot 10^3$	10^3	$1 \cdot 3 \cdot 10^{-4}$	$H + O_3 \rightarrow OH + O_2$ $HO_2 + O \rightarrow OH + O_2$	
O O O	$^3P_1 \rightarrow {}^3P_2$ $^3P_0 \rightarrow {}^3P_1$	63.09 147.06	100–>200*				Thermally excited	

* Produces heating between 80–100 km

and infrared can not be determined to the desired accuracy, and measurements from high flying aircraft and space platforms outside the atmosphere suffer from inadequate control of their absolute calibration.

Two major programs have been carried out in the past which started from different points of view. Labs and Neckel [61, 62] made carefully calibrated high spatial resolution measurements of the solar *radiance* at the center of the sun from the ground (Jungfraujoch, 3,500 m) and corrected the measurements for solar limb darkening and atmospheric attenuation. Thekaekara [63, 64] evaluated measurements of the spectral solar *irradiance* made from high altitude aircrafts, balloons and space platforms. In these experiments attempts have been made to measure the radiation flux from the whole sun at 1 Astronomical Unit, the mean radius of the earth's orbit.

The state of the art of solar spectral irradiance measurements was reviewed at a workshop and a symposium held in Washington [65, 220], by White [66a], and more recently by London and Fröhlich [66b]. A proposed standard curve of solar spectral irradiance as deduced by Thekaekara is referred to in different publications [67, 68, 69], where the interested reader will find the data in tabulated form. Two words of caution in using these data are necessary:

a) The discrepancy between the proposed spectral distributions and that one of Labs and Neckel in their narrower spectral interval (401–657 nm) is not yet resolved, and
b) the proposed spectral distributions are normalized to a solar constant of 1,353 Wm^{-2} which is probably 15–17 Wm^{-2} too small.

The Fig. 10 presents the short wave part of the spectrum in graphical form together with the penetration depth into the atmosphere.

For the solar spectral irradiance at the top of the earth atmosphere in 1 Astronomical Unit (A.U.) $= 1.496 \cdot 10^{11}$ m distance from the sun the symbol $S_{0,\lambda}$ is introduced. 1 A.U. is the mean radius of the earth orbit around the sun. The total flux

$$S_0 = \int_0^\infty S_{0,\lambda} d\lambda = 1370 \text{ Wm}^{-2} \tag{96}$$

is called *Solar Constant* and will be discussed later.

The electromagnetic wave energy reaching the earth orbit at mean distance from the sun per unit area is traditionally called the Solar Constant (S_0) though it is not a constant in a physical sense. The solar electromagnetic radiation is not produced by a simple black body emission but is generated in different layers of the solar atmosphere which has a wide temperature range. Far infrared radiation around 100 μm wavelength is emitted by the relatively cold upper photosphere with a temperature range of 4,150–4,450 K. The near infrared emission indicates temperatures between 6,000 and about 6,700 K. The maximum, around 1.6 μm, originates in the deepest observable layers of the solar atmosphere. The visible part of the spectrum can be approximated by a 6,000 K black body radiation which corresponds to temperatures in the middle photosphere. This part of the spectrum is, however, modified by the absorption of gases in the higher and colder layers of the photosphere which causes the dark Fraunhofer lines. In the optically

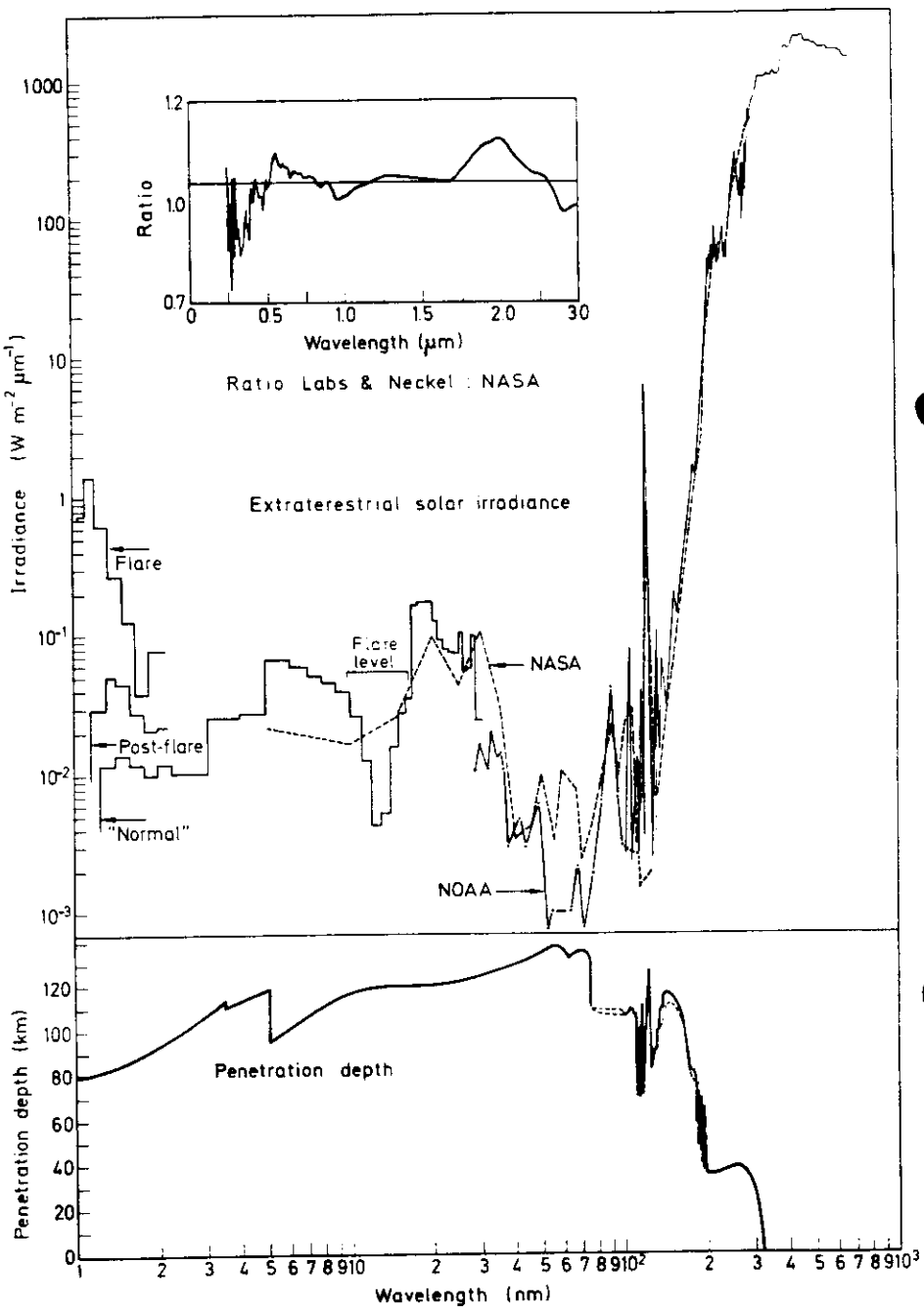

Fig. 10. Solar irradiance at the top of the atmosphere at 1 A.U. distance between sun and earth after NASA [67] and NOAA [69]. Lower part: penetration depth for which the radiance is attenuated to 1/e. (After Friedman [70])

thin cromosphere temperatures rise again to several ten – to hundred thousand degrees which produce lines from ionized atoms in the shortwave ultraviolett [70]. Finally in the corona the temperatures are larger than 10^6K.

Attenuation of Solar Radiation in the Atmosphere

The spectral Rayleigh scattering coefficient $\sigma_R(\lambda)$ was derived earlier [Eq. (26)] and defines the attenuation per unit length. In Table 6 some values are presented for the conditions at the bottom of a mid latitude standard atmosphere ($T=288.15$ K, $p=1.01325 \cdot 10^5$ Pa) according to [18]. In order to determine the optical path through the whole atmosphere one has, in principle, to integrate Eq. (21) from the top to the bottom of the atmosphere along the line of sight.

In order to derive a formula for the atmospheric transmission let us assume that the sun is located at a zenith angle ζ. Until it reaches the ground the solar radiation has to pass a larger air mass then for vertical incidence. A *relative airmass* M (ζ) can be defined which gives the ratio of the airmass traversed under the zenith angle ζ to vertical incidence. Because of the curvature of the earth and refraction the relative airmass is a complicated function of the zenith angle [71, 72].

Table 6. Rayleigh scattering coefficient, optical depth and transmittance as well as the turbidity factor for a mid latitude standard atmosphere [18]

Wavelength in μm	Rayleigh scattering coefficient at STP in m^{-1}	$T(\lambda)$	Rayleigh optical depth $\delta_R(\lambda)$	Transmission due to Rayleigh scattering only	
				$\zeta_\odot = 0$	$\zeta_\odot = 75$
0.27	$2.282 \cdot 10^{-4}$	(38)	1.9314	0.1449	0.00057
0.28	$1.948 \cdot 10^{-4}$	(23)	1.6481	0.1924	0.00172
0.30	$1.446 \cdot 10^{-4}$	(4.06)	1.2237	0.2941	0.0209
0.32	$1.089 \cdot 10^{-4}$	(1.67)	0.9290	0.3949	0.0276
0.34	$8.494 \cdot 10^{-5}$	(1.46)	0.7188	0.4873	0.0622
0.36	$6.680 \cdot 10^{-5}$	(1.54)	0.5653	0.5682	0.1126
0.38	$5.327 \cdot 10^{-5}$	1.65	0.4508	0.6371	0.1752
0.40	$4.303 \cdot 10^{-5}$	1.70	0.3641	0.6948	0.2449
0.45	$2.641 \cdot 10^{-5}$	2.03	0.2238	0.7995	0.4212
0.50	$1.726 \cdot 10^{-5}$	2.55	0.1452	0.8648	0.5706
0.55	$1.162 \cdot 10^{-5}$	(3.36)	0.0984	0.9063	0.6837
0.60	$8.157 \cdot 10^{-6}$	(4.42)	0.0690	0.9333	0.7660
0.65	$5.893 \cdot 10^{-6}$	(5.05)	0.0499	0.9513	0.8246
0.70	$4.364 \cdot 10^{-6}$	(5.88)	0.0369	0.9638	0.8671
0.80	$2.545 \cdot 10^{-6}$	(8.70)	0.0215	0.9787	0.9203
0.90	$1.583 \cdot 10^{-6}$	12.48	0.0134	0.9867	0.9495
1.06	$8.458 \cdot 10^{-7}$	21.0	0.0072	0.9928	0.9726
1.26	$4.076 \cdot 10^{-7}$	41.5	0.0034	0.9966	0.9869
1.67	$1.327 \cdot 10^{-7}$	114	0.0011	0.9989	0.9958
2.17	$4.586 \cdot 10^{-8}$	273	0.0004	0.9996	0.9985
3.50	$6.830 \cdot 10^{-9}$	890	0.0001	0.9999	0.9996
4.00	$4.002 \cdot 10^{-9}$				

Table 7. Relative air (M) and water vapor (M_w) masses in dependence of the zenith angle ζ

ζ =	75	80	81	82	83	84	85	86	87	88	89	90°
$M(\zeta)$ =	3.81	5.59	6.16	6.86	7.73	8.85	10.32	12.33	15.18	19.46	26.31	36.26
$M_w(\zeta)$ =	3.85	5.71	6.33	7.09	8.07	9.35	11.1	13.7	17.6	24.5	38.6	75.1

However, for $\zeta \leq 80°$ it can be approximated by

$$M(\zeta) \cong \frac{1}{\cos \zeta} = \frac{1}{\mu}. \tag{97}$$

For $\zeta \geq 75°$ the correct values are given in Table 7.

In this table also the relative water vapor mass $M_w(\zeta)$ has been included. Because of the different height distribution of water vapor the *sec* ξ condition holds much closer.

The transmission of the atmosphere can now be described by the general formula

$$\tau = e^{-\delta M(\zeta)} = e^{-\delta_R T M(\zeta)}, \tag{98}$$

where δ is the total optical depth of the atmosphere for vertical incidence (sun in zenith), and δ_R the respective value for Rayleigh scattering. T is the "turbidity factor" introduced by Linke [73]. In the formulation of Eq. (98) it is assumed that the transmittance can be computed from the molecular scattering approximation if the optical path is prolonged by a factor T. T is essentially the number of Rayleigh atmospheres which have to be put on top of each other in order to produce the same extinction as the turbid atmosphere.

Equation (98) can first be considered for narrow, nearly monochromatic spectral bands. In this case the spectral optical depth and the spectral turbidity factor $T(\lambda)$ have to be used in the computations. Typical values of $T(\lambda)$ for a clear standard atmosphere are also given in Table 6. The values in parenthesis are for spectral regions in which atmospheric gaseous absorption is present (mainly ozone). It can be seen that the turbidity factor increases rapidly towards longer wavelengths because of the much different wavelength behavior of molecular and aerosol scattering. The molecular scattering decreases proportional $\lambda^{-4.09}$ and the aerosol scattering proportional $\sim \lambda^{-1.5}$. The various effects which contribute to the attenuation of the solar radiation are schematically presented in Fig. 11. Since the molecular scattering can easily be computed from the known Rayleigh scattering coefficient Eq. (26), a measurement of the spectral transmittance in combination with Eq. (98) provides a measure for T, the turbidity of the atmosphere.

Measurements of the spectral atmospheric transmittance are of high practical value for pollution monitoring. From these measurements not only can the total aerosol load of the atmosphere be deduced but also information about its size distribution be derived. The scattering efficiency at a specified wavelength of aerosols depends on its size distribution. Therefore the spectral dependence

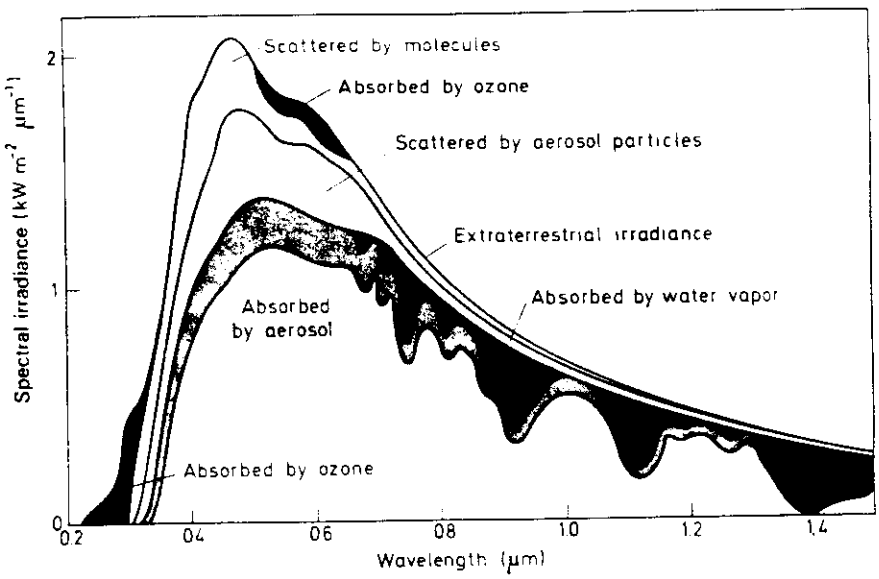

Fig. 11. Attenuation processes for solar radiance in a cloudfree atmosphere (After Quenzel [74])

of the scattering coefficient contains information on this size distribution which can be inferred by the application of mathematical inversion methods [75, 76].

By integration over the whole solar spectrum the spectrally averaged turbidity factor can be deduced. It has, however, to be taken into account that ozone and water vapor also absorb and thus contribute to the extinction (turbidity values contaminated by water vapor or ozone absorption are put into parenthesis in Table 6). Furthermore the Rayleigh optical depth gets dependent on the zenith angle of the sun because with increasing zenith angle the transmitted solar spectrum is shifted towards longer wavelength according to the wavelength dependence of the scattering coefficient (see next section).

To arrive at reliable aerosol turbidity values from total solar radiation measurements is not a straight foreward procedure and requires experience (see e.g. Robinson [77]). Some guiding values after Schulze [78] are:

High Mountain area	$T=1.9$
Rural Lowland	$T=2.75$
Large cities	$T=3.75$
Industrial area, highly polluted	$T=5.0$.

More detailed data are given by Linke [73].

In a cloudfree atmosphere with low turbidity the daily average transmission varies over the year between 0.84 and 0.93. The average relative irradiance is 0.77 ± 0.01 at the equator with a mean solar zenith angle of $\zeta = 52.3°$, and varies between zero (polar night) and 0.69 at the poles.

Deduction of the Formula for the Transmittance of a Scattering Atmosphere

We consider the sun to be at zenith angle ζ.

Instead of the geometrical path s through the atmosphere the vertical height z can be introduced and with the relative air man $M(\zeta)$ the geometrical path becomes

$$\mathrm{d}s = M(\zeta)\,\mathrm{d}z. \tag{99}$$

Using Eq. (99) the optical path $u_R(\lambda, \zeta; z_0, z_\infty)$ through the whole atmosphere can be expressed for molecular scattering by

$$u_R(\lambda, \zeta; 0, \infty) = \int_0^\infty \sigma_R(\lambda, z)\, M(\zeta)\,\mathrm{d}z, \tag{100}$$

where $\sigma_R(\lambda, z)$ is the Rayleigh scattering coefficient for the pressure and temperature conditions at z.

The Rayleigh scattering coefficient is defined by Eq. (26) for N scattering centers per unit volume. The number of molecules is defined by the equation of state for an ideal gas

$$N = p/kT = N_A p/RT = 7.243 \cdot 10^{22}\,\frac{p}{T}\,\frac{\mathrm{Pa}}{\mathrm{J}} \tag{101}$$

$N_A = 6.022 \cdot 10^{23}\ \mathrm{mol}^{-1}$ is the number of molecules per mol (Avogadro's number). $R = 8.314\ \mathrm{J\ mol^{-1}\ K^{-1}}$ the molar gas constant and T the absolute temperature.

The formula for the Rayleigh scattering coefficient is therefore in terms of pressure and temperature given by

$$\sigma_R(\lambda) = \frac{32\pi^3 (n-1)^2 T}{2.1729 \cdot 10^{25}\, p\, \lambda^4}. \tag{102}$$

λ in m.

For $p = 10^5$ Pa, $T = 273.15$ K and $(n-1)$ computed after Eq. (31) it results for $\lambda = 550$ nm

$$\sigma_R(550\ \mathrm{nm}) = \frac{32\pi^3 (2.911 \cdot 10^{-4})^2 \cdot 273.15}{3 \cdot 7.243.10^{22} \cdot 10^5 (0.55 \cdot 10^{-6})^4} = 1.16 \cdot 10^{-5}\ \mathrm{m}^{-1}. \tag{103}$$

Let us assume vertical incidence ($\mu = 1$) first. In this case the symbol δ is introduced for the vertical optical path

$$\delta_R(\lambda; 0) = u_R(\lambda, \zeta = 0; 0, \infty) \tag{104}$$

which is called the *optical depth* of the atmosphere. More generally

$$\delta(\lambda; z) = u(\lambda, \zeta = 0; z, \infty) \tag{105}$$

is the optical depth of the atmosphere at the altitude z.

The optical depth of the entire atmosphere due to Rayleigh scattering.

$$\delta_R(\lambda, 0) = -\int_0^\infty \sigma_R(\lambda, z)\,\mathrm{d}z, \tag{106}$$

can in good approximation (about 1.5% error) be expressed by the value $\sigma_R(\lambda, 0)$ at STP conditions and the equivalent height H of the atmosphere which would be its vertical extent if the whole atmosphere is compressed to 0.1013 MPa pressure at 273 K:

$$\delta_R(\lambda, 0) \cong \sigma_R(\lambda, 0)\, H. \tag{107}$$

H is the *scale height* of the atmosphere and can be computed from the hydrostatic equation $g\varrho\mathrm{d}z = -\mathrm{d}p$ and the state equation of an ideal gas, $p = \varrho \frac{RT}{M_a}$, as

$$H = \frac{RT_0}{M_a g} \cong 8{,}000\ \mathrm{m} \tag{108}$$

($R = 8.314\ \mathrm{J\ mol^{-1}\ K^{-1}}$, molar gas constant; $T_0 = 273.15$ K; $M_a = 0.028964\ \mathrm{kg\ mol^{-1}}$, molar mass of air up to about 90 km; $g = 9.8062\ \mathrm{m\ s^{-1}}$, acceleration due to gravity at 45° latitude).

With $\sigma_R(550\text{ nm}, 0) = 1.162 \cdot 10^{-5}\,\text{m}^{-1}$ from Table 6 and the value of H from Eq. (108) the optical depth of the atmosphere due to Rayleigh scattering at 550 nm is according to Eq. (107)

$$\delta_R(550\text{ nm}, 0) \cong 0.093 \tag{109}$$

which is equivalent to a transmittance of

$$\tau_R(550\text{ nm}, M(\zeta) = 1; 0, \infty) = e^{-0.093} = 0.91. \tag{110}$$

Thus 9% of the energy is scattered out of the direct beam.

The transmittance for an inclined beam is according to Eq. (100)

$$\tau_R(\lambda, \zeta; z, \infty) = e^{-\delta_R(\lambda, z) M(\zeta)}. \tag{111}$$

Values for the Rayleigh optical depth and transmittances for $M(\zeta) = 1$ and $M(\zeta) = 3.82$ presented in Table 6 have been computed for a mid latitude standard atmosphere ($T_0 = 288.15$ K) under consideration of the true temperature profile [18].

Now the spectral irradiance of the sun at the earth surface under normal incidence can be computed by application of Eq. (111):

$$S_\lambda(z = 0) = S_{0,\lambda} e^{-\delta_R(\lambda, 0) M(\zeta)}. \tag{112}$$

The total solar irradiance for a zenith angle $\neq 0$ at the horizontal earth surface, $E_\odot$, can be obtained from Eq. (112) by multiplication of the unit area by $\cos \zeta_0 = \mu$ and integration over all wavelengths.

$$E_\odot(\mu) = \mu \int_0^\infty S_{0,\lambda} e^{-\delta_R(\lambda, 0) M(\zeta)} d\lambda = \mu S_0 \tau_R'. \tag{113}$$

As indicated in Eq. (113) it is desirable to express the solar irradiance at the surface by the solar constant defined by Eq. (96) and an integrated transmittance $\tau_R'(\delta)$

$$\tau_R' = e^{-\delta_R M(\zeta)} = \int_0^\infty \frac{S_{0,\lambda}}{S_0} e^{-\delta_R(\lambda, 0) M(\zeta)} d\lambda. \tag{114}$$

Due to this definition the spectrally integrated optical depth δ_R becomes dependent on the relative air mass $M(\zeta)$. Numerical integration of equation (114) leads to the following representation of δ_R:

$$\delta_R[M(\zeta)] = \delta_R(1) \cdot P(\zeta). \tag{115}$$

Values obtained for $P(\zeta)$ are given in Table 8.

With increasing zenith angle the spectrally averaged and vertically measured optical Rayleigh depth of the atmosphere decreases because in the spectral distribution of the transmitted radiation the longer wavelengths where more energy is contained (compare Fig. 10) are favoured due to the $\lambda^{-4.09}$ dependence of the Rayleigh scattering coefficient. The spectrally integrated optical depth for vertical incidence [$M(\zeta) = 1$] has the numerical value $\delta_R(1) = 0.0992$ which results in a transmittance of $\tau = 0.906$.

Aerosol extinction can be included in the computation by generalizing e.g. Eqs. (111) and (106) to

$$\tau(\lambda, \zeta; z, \infty) = \exp\left\{-\int_z^\infty [\sigma_R(\lambda, z') M(\zeta, z') + \sigma_M(\lambda, z') M_M(\zeta, z')]\, dz'\right\}. \tag{116}$$

Because of the different vertical distributions the relative air mass for aerosols is not exactly the same as for molecules. Also $M(\zeta)$ is not constant with height because of the curvature of the earth (see Fig. 12). Again for angles $\zeta < 75°$, $M(\zeta, z) = M_M(\zeta, z) = \sec \zeta$ is a sufficiently good approximation. Then

Table 8. Values of the reduction factor $P(\zeta)$ defined by Eq. (115) in dependence of the relative air mass $M(\zeta)$

$M(\zeta)$	0.5	1.0	1.5	2	3	4	6	8	10
$P(\zeta)$	1.058	1.0	0.949	0.900	0.826	0.768	0.675	0.608	0.555

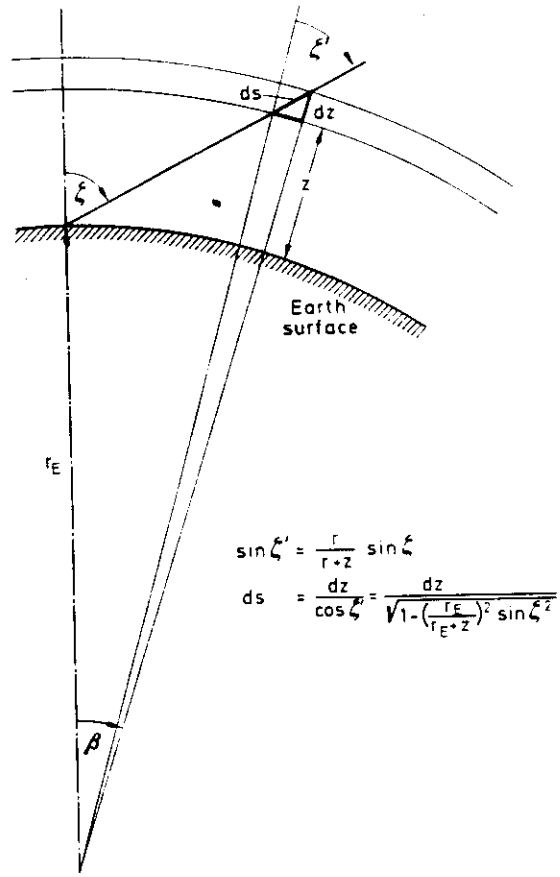

Fig. 12. Optical path in a spherical atmosphere

it may be written (under omission of the spectral index):

$$\sigma_R + \sigma_M = \sigma_R\left(1+\frac{\sigma_M}{\sigma_R}\right) = T\sigma_R. \tag{117}$$

T is the *turbidity factor* introduced by Linke [73]. It can be computed spectrally from Eqs. (26) and (65) if the aerosol content and its size distribution are known. It can also directly be deduced from measured transmittances since the Rayleigh scattering coefficient can easily be computed. From Eq. (116) it would follow with $M_M = M$: $T = -\ln\tau/\delta_R M(\zeta)$.

However, in this case the turbidity factor would include the effects of absorbing gases. More generally Eq. (116) has to be written:

$$\tau(\zeta; z, \infty) = \exp\{-(\delta_R(z)T + \delta_{O_3}(z) + \delta_{H_2O}(z))\mu^{-1}\}, \tag{118}$$

where the $\delta(z)$ denote the spectrally integrated optical depths of the whole atmosphere down to a level z. Only if the ozone and water vapor absorptions are known (there is also a small absorption of O_2 involved), it is possible to determine the turbidity factor from

$$T = -\frac{1}{\delta_R}(\mu\ln\tau + \delta_{O_3} + \delta_{H_2O}). \tag{119}$$

Scattered Solar Radiation

Single Rayleigh scattering, according to it symmetrical phase function, scatters the same amount of solar radiation back to space as in the direction of the earth surface. If S_0 is the solar constant and $E_\odot(\infty)=S_0\cos\zeta_\odot$ the irradiance at the top of the atmosphere, then the fraction

$$E_\odot(0)/E_\odot(\infty)=\exp\{-T\sigma_R HM(\zeta)\} \tag{120}$$

arrives at the horizontal earth surface. H is the height of the homogenous atmosphere defined by Eq. (108). The fractional total scattered radiation in a non-absorbing atmosphere over a black earth surface would then be

$$1-e^{-T\sigma_R HM(\zeta_\odot)}.$$

A fraction q is scattered toward the earth, generating an irradiance of diffuse radiation of

$$E_d=qS_0\cos\zeta_\odot(1-e^{-T\sigma_R HM(\zeta_\odot)}). \tag{121}$$

In a cloudfree atmosphere according to Berlage [79] 50% of the scattered radiation is directed towards the earth surface, 50% are lost to space. If $\tau[M(\zeta_\odot)]$ is the transmission of the atmosphere at airmass $M(\zeta_\odot)$, then the diffuse scattered radiation is

$$E_d=0.5\,S_0\cos\zeta_\odot[1-\tau(\zeta_\odot, T)]. \tag{122}$$

For a Rayleigh atmosphere $q=0.5$ is still a good approximation ($\sim 1\%$) even if multiple scattering is accounted for. In the case of a turbid atmosphere one would expect that because of the stronger forward scattering the factor q will be larger. However, due to multiple scattering this effect is largely compensated.

If one accounts also for the absorption by aerosol, water vapor and ozone in the atmosphere by introduction of the extinction factor $aHM(\zeta_\odot)$ the formula

$$E_d=0.5\,S_0\cos\zeta_\odot e^{-a_\cdot HM(\zeta_\odot)}(1-e^{-T\sigma_R H/\cos\zeta_\odot}) \tag{123}$$

represents with reasonable accuracy the irradiance by diffuse clear sky radiation at the horizontal surface of the earth [78]. Different experimental investigations [80, 81] lead to the result, that the absorption contributes 10–20% to the total extinction by aerosols. The absorbed radiant energy heats the atmosphere.

The differences in the scattering properties of different air masses can be seen in Fig. 13. Here the zenith radiance is plotted in dependence of the wavelength normalized at 780 nm for the city of Munich at solar zenith angles of 37.3° and 59.0° and for a coastal station in the Mediterranean region at a solar zenith angle of about 43° which is in-between the two values of Munich. It can clearly be seen that the slope of the spectrum for the Mediterranean station is steeper but strong variations occur also in the urban atmosphere. In addition a measurement from a mountain station (Jungfraujoch, 3,570 m) is added which has an even steeper decrease towards longer wavelengths but still not the slope for Rayleigh scattering as indicated by the curve R is reached. In the polluted urban atmosphere there is a tendency towards a more shallow slope in the spectral distribution especially at shorter wavelengths, which is a consequence of the larger aerosol concentration.

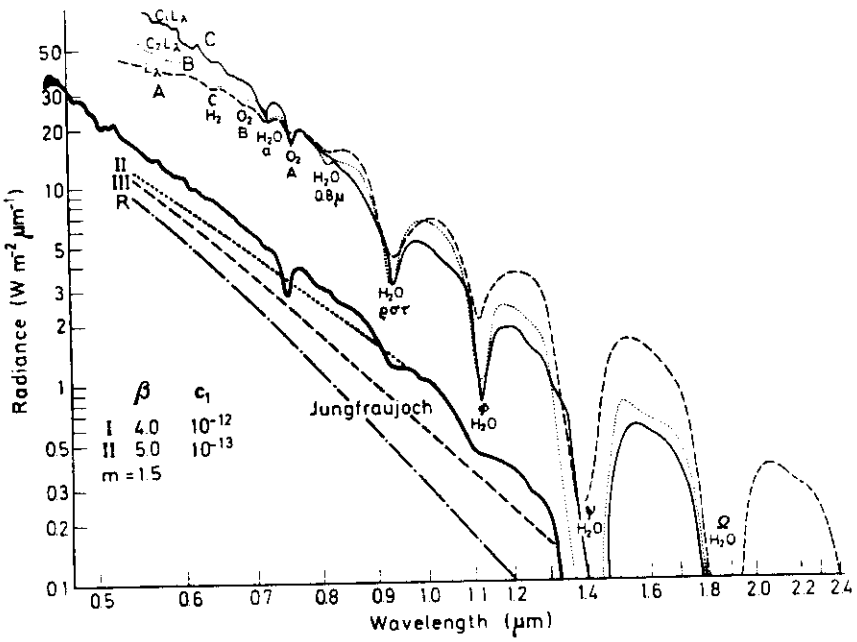

Fig. 13. Spectral zenith radiance of scattered solar radiation A: Absolute radiance observed in Munich, 25. July 1962, $\zeta_\odot = 38°$. B: Radiance observed in Munich, 2. October 1962, $\zeta_\odot = 59°$, normalized to spectrum A at 780 nm. C: Radiance observed in S. Agata sui due golfi, $\varphi = 40°37'$N, $\lambda = 14°11'$E, 19 August 1961, normalized to spectrum A, at 780 nm, D: Absolute radiance observed at Jungfraujoch (3570 m), February 1961. R: Theoretical Rayleigh scattering curve for Munich. II, III: Radiance computed for Mie scattering. (After Bolle et al. [82])

Strong foreward scattering is reflected in high radiance values around the sun. The minimum occurs at about 90° off the direction of the sun. Towards the horizon the radiance increases because of the increasing air mass. This has often been measured [82] and can also be computed by application of a rigorous radiation transfer theory as we shall see later (compare Fig. 23).

Atmospheric Longwave Radiation

The radiation which is emitted by the atmosphere and the earth surface due to the temperature structure in the atmosphere-surface system is governed by the Planck function, Eqs. (86) and (87), and the distribution of emitting gases and aerosols in the atmosphere. For the temperature range which exist in the layers emitting at LTE (180–330 K) the emission starts to reach measurable values at about 2.5 μm and extends through the whole infrared to the mm region. The maximum spectral radiance values *per unit wavelength interval* occur around 10 μm wavelength (around 600 cm^{-1} if plotted per unit wavenumber interval).

The transition between scattered solar radiation and infrared radiation emitted by the atmosphere can be recognized in Fig. 14. In its lower part at the left side the zenith radiance of scattered solar radiation of the clear sky is reproduced

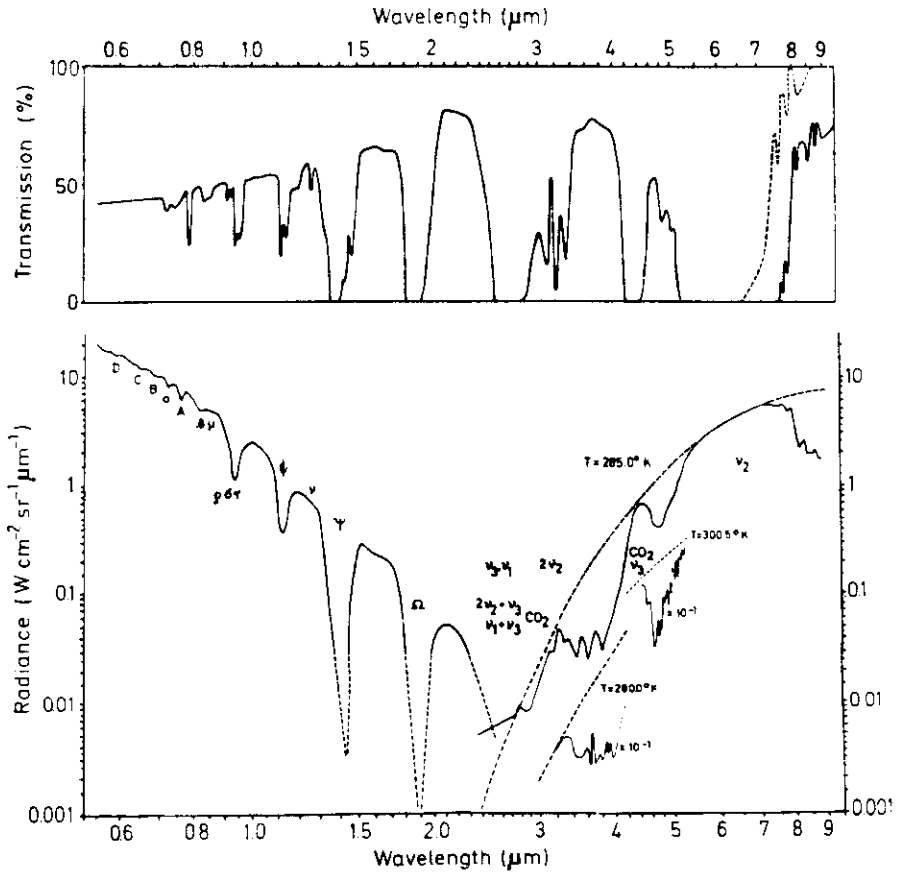

Fig. 14. Atmospheric spectrum 0.5–9 μm. Upper part: Transmission through a horizontal atmospheric path of 5,500 m with 1.37 g cm^{-2} water vapor (dashed line 300 m path with 0.11 g cm^{-2} H_2O) (After Yates and Tylor [83]). Lower part: Zenith spectral radiance of scattered solar radiation and emitted atmospheric radiation. (After Bolle [84])

with the slope already known from Fig. 13. Near 2.5 μm the emission of atmospheric gases starts to overlap the scattered radiance and increases towards longer wavelengths. In strong vibration-rotation bands like the CO_2 band at 4.3 μm and the water vapor band at 6.3 μm (compare Table 2a) the emission reaches the Planckian Function (dashed curve) for the air temperature near the surface (285 K). The structure in the "windows" at 3.8 and 4.8 μm as observed under higher spectral resolution can be seen in the displaced inserts as measured at other occasions [85, 86]. In the upper part of Fig. 14 the atmospheric transmission measured by Yates and Taylor [83] is plotted for comparison. The bands denoted by letters in the scattered solar spectrum are identified as follows:

A	O_2 (0–0)	0.7621 μm	D	NaI	0.58899 μm
B	O_2 (0–1)	0.6884 μm			0.58959 μm.
C	H_α	0.65628 μm	H_2O bauds compare Tables 2c and 10		

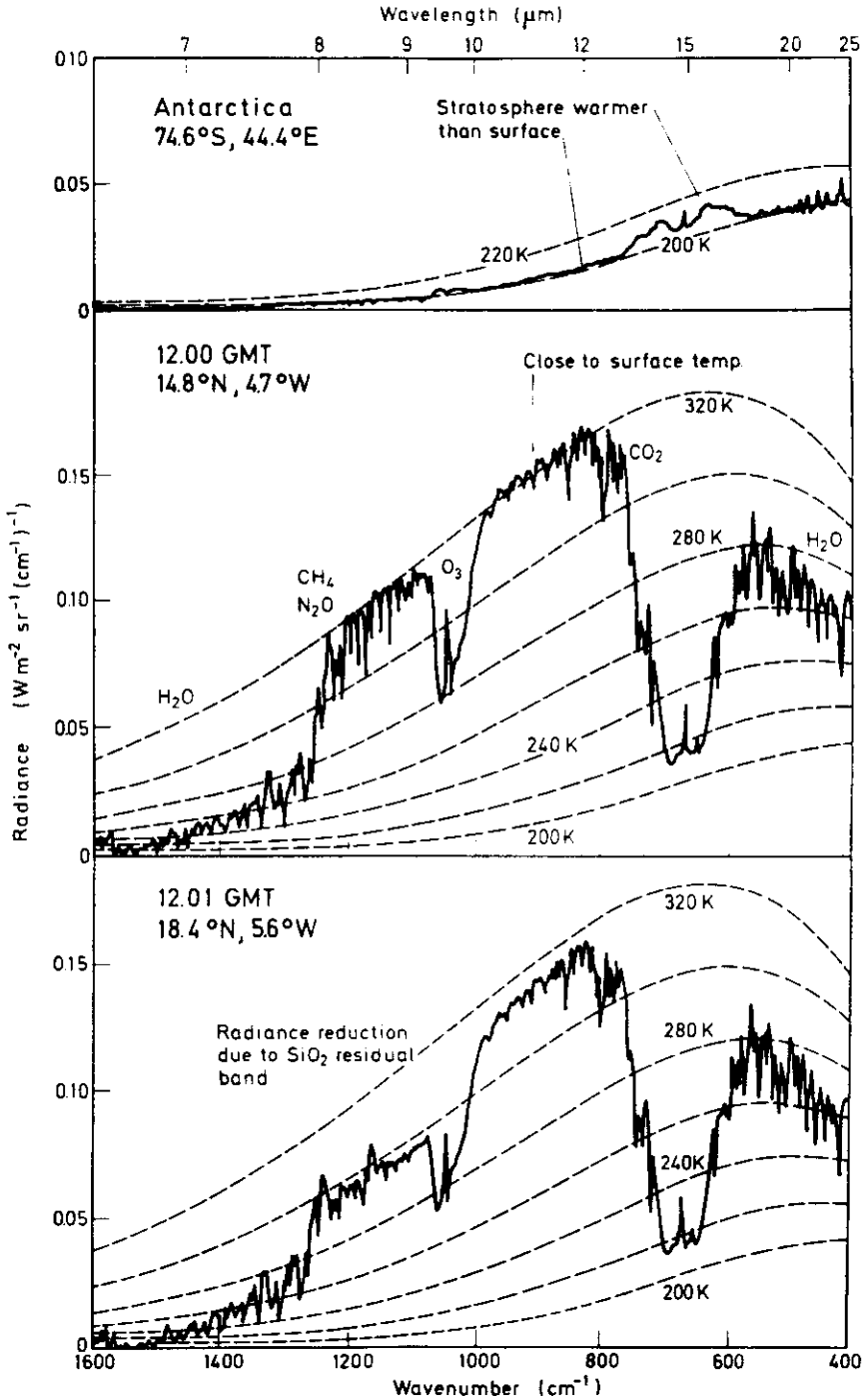

Fig. 15. The terrestrial emission spectrum as measured from space. (After Hanel et al. [87])

The variability of the atmospheric emission is beside of the temperature primarely produced by the variable water vapor mass. The contributions by CO_2 and some other minor constituents such as N_2O and CH_4 (compare Table 2a) are much more constant; but are not unimportant for the discussion on climate effects of changing trace gas concentrations as discussed in a later section. O_3 emits only in a small fraction of the whole spectrum between 9 and 10 μm and around 14 μm. Its concentration varies by about ±30% over the globe.

Hanel [87] has made spectral measurements of the longwave radiation emerging from the top of the atmosphere from the satellite NIMBUS-5. These spectra provide an excellent survey on the interrelation between the emission of the earth's surface and the atmospheric gases (Fig. 15). The emission of the atmosphere measured from the ground in different locations in the same spectral interval is shown in Fig. 16. Beyond 15 μm the spectrum is entirely determined by the rotational band of water vapor (compare Fig. 7). There it exists nearly no transparency between ground and space, except under extremely dry conditions or at elevated sites.

At LTE (local thermodynamic equilibrium) each volume element radiates isotropically into all directions. Therefore the radiation emitted by the system does not have the strong azimuth dependence as observed especially at large solar zenith angles for scattered solar radiation. Variations in azimuth are only observed if the water vapor and aerosol distribution is not horizontally homogenous [84]. The observed radiance depends therefore primarely on the zenith angle of observation according to the radiating air mass [84].

The basic approaches to compute the distribution of far infrared radiances and long wave radiation fluxes are discussed in a later section.

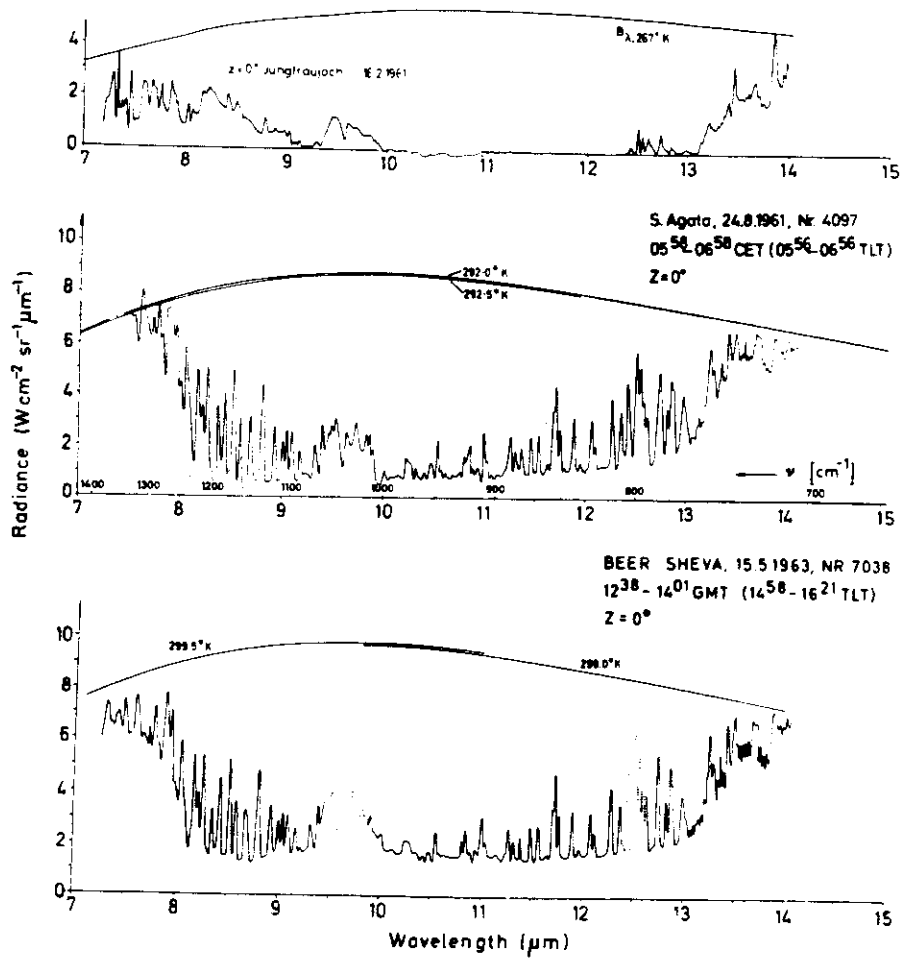

Fig. 16. The atmospheric zenith emission spectrum between 7 and 15 μm as measured in three locations. (After Bolle [84]). Top: Jungfraujoch, Switzerland, 3,570 m altitude, 16.2.1961. Middle: S. Agata sue due golfi, Italy, 24.8.1961, 05:56–06:56 TLT. Bottom: Beer Sheva, Israel, 15.5.1963, 14:58–16:21 TLT

If a geometrical path along the direction s is considered at the height z in the atmosphere, the radiance can be denoted by $L(z; s)$ in a horizontally homogenous atmosphere. The direction s can be expressed by the zenith angle ζ and the azimuth φ. As vertical coordinate the optical depth of the atmosphere, $\delta = \int \sigma_e \, dz$, will be used. The increment of the geometrical path, ds, will be replaced by $ds = \frac{d\delta}{\sigma_e \mu}$, where $\mu = \cos\zeta$. The radiance $L(\delta; \varphi, \mu)$ is attenuated due to extinction between s and $s + ds$ by the amount

$$\{dL(\delta; \varphi, \mu)\}_{ext} = -L(\delta; \varphi, \mu) \frac{d\delta}{\mu}. \tag{131}$$

It will on the other hand be increased due to scatter from other directions s' into the direction s and/or by emission according to

$$\{dL(\delta; \varphi, \mu)\}_{add} = \tilde{J}(\delta; \varphi, \mu; \varphi', \mu') \frac{d\delta}{\sigma_e \mu} \tag{132}$$

where $J(\delta; \varphi, \mu; \varphi', \mu') = \sigma_e^{-1} \tilde{J}(\delta; \varphi, \mu; \varphi', \mu')$ is the *source function* for this additional radiance. The total change in L is the sum of Eqs. (133) and (132) which can be written after division by $d\delta \, \mu$:

$$\mu \frac{dL(\delta; \varphi, \mu)}{d\delta} = -L(\delta; \varphi, \mu) + J(\delta; \varphi, \mu; \varphi', \mu'). \tag{133}$$

Equation (133) is the general radiative transfer equation (RTE), which applies to all radiation problems. The sign of the l.h.s. depends on the choice of the positive direction for s.

The Source Function for a Scattering Atmosphere

The source function can be derived from an inspection of the involved process. For the moment only scattering and absorption in aerosols will be considered. In this case the incremental radiance emerging from a small volume in the direction φ, μ results from scattering of radiation which traverses the volume in all other directions. Consider a direction φ', μ' in which the radiance $L(\delta; \varphi', \mu')$ proceeds within a solid angle $d\Omega'$. This radiance generates a scattered radiance $dL(\delta; \varphi, \mu; \varphi', \mu')$ in the direction φ, μ within the incremental solid angle $d\Omega$ of the magnitude

$$\{d^2 L(\delta; \varphi, \mu; \varphi', \mu') d\Omega\}_{sc} = \sigma L(\delta; \varphi', \mu') \cdot p(\delta; \varphi, \mu; \varphi', \mu') \frac{d\Omega'}{4\pi} \frac{d\delta}{\sigma_e \mu} d\Omega. \tag{134}$$

Here $p(\delta; \varphi, \mu; \varphi', \mu')$ is the scattering phase function defined in Eq. (27) which prescribes the distribution of the scattered radiation $\sigma L(\delta; \varphi, \mu')$ to the different directions, $d\Omega'/4\pi$ is the ratio of the incremental solid angle to the sphere from where the radiation comes and $d\Omega$ is the small solid angle into which the radiation is scattered. The geometrical path ds in which the scattering occurs is again expressed by $d\delta/\sigma_e \mu$. According to Eq. (5b) $\sigma/\sigma_e = \tilde{\omega}$ is the single scattering albedo, and for the scattering phase function the normalization

$$\frac{1}{4\pi} \int p(\delta; \varphi, \mu; \varphi', \mu') \, d\Omega = \tilde{\omega} = \frac{\sigma}{\sigma_e} \leqq 1 \tag{135}$$

applies.

In order to account for all directions from where radiation arrives in the scattering volume, Eq. (134) has to be integrated over all solid angles $d\Omega'$ which results in

$$\left\{\mu \frac{dL(\delta; \varphi, \mu)}{d\delta}\right\}_{sc} = \frac{\tilde{\omega}}{4\pi} \left(\int_{4\pi\Omega_0} L(\delta; \varphi', \mu') \cdot p(\delta; \varphi, \mu; \varphi', \mu') \, d\Omega' \right). \tag{136}$$

By comparison with Eq. (133) one can see that the r.h.s. of equation (136) is the source function J for this process.

It can be seen that the solution of the radiative transfer equation is complicated by the scattering properties of aerosols.

Especially if large particles contribute to the scattered radiance the computation of the integral in (136) is difficult to perform because of the strong forward peak in the scattered radiance.

Methods to Compute Radiances and Fluxes in a Turbid Atmosphere

In order to get the radiance at any point and in all directions, Eq. (133) has further to be integrated over the whole atmosphere and all higher orders of scattering have to be regarded, including reflection at the ground.

There exist different methods to solve the RTE which have recently be reviewed by Lenoble et al. [149, 150], and which can only shortly be described and referenced here.

Monte Carlo Method [151–155]

In this method the path of one photon after another is computed assuming a random chain of scattering and/or absorption processes. After a large number (e.g. 10^6) of photons has been tracked the number of photons arriving at the detector are counted and set into relation to the initial number.

Approximation by Spherical harmonics [156–158]

The phase function is first separated in azimuth by expansion in Fourier series mostly by the use of Legrendre polynomials. Then the radiation transfer equation is expressed in Legendre functions and a System of first order linear differential equations results for the coefficients of the expansion which has to be solved.

Method of Discrete Ordinates [159–162]

The equation of radiative transfer is separated in azimuth and the integrals replaced by sums. A set of first-order nonhomogeneous differential equation is generated which can be solved numerically.

Gauss-Seidel Iteration [163–166]

The atmosphere is divided into layers and the unit sphere into a set of solid angle increments. Thus the optical depth and he solid angle are discretized and the radiative transfer equation is approximated by a set of linear algebraic equations.

Method of Successive Orders of Scattering [167–171]

The intensity is expressed as a series developed for the number of scattering processes to be considered. Then the equation of radiative transfer is solved after separation in azimuth.

Discrete Space Theory (Matrix Operator Method) [172–176]

The laws for transmission, reflection and absorption (interaction principle) are formulated for discrete layers of the atmosphere. Reflectivity and transmissivity are represented by matrix operators. From the formulation for one layer the method is extended to two and more layers by applying matrix multiplication formalism.

Doubling or Adding Method [177–184]

The reflection and transmission of each of two layers are considered as known. Then the reflection and transmission of the two layers together can be obtained by computing the back-and-forth reflections between the two layers. If the initial thin layers are of equal depth the result for a thick layer can be build up by geometrically adding two layers of equal depth.

Invariance Principle [184, 185]

This is another method where like in the case of Monte Carlo computations no direct attempt is made to solve the radiation transfer equation. A number of logical relations are defined which relate upwards and downwards directed irradiances by means of generally defined transmission and reflection functions to each other. These are the invariant relations, which are differentiated for the optical depth and the derivatives are eliminated by means of the radiative transfer equation which enters as a side relation. The generated system of equations is solved by expanding the scattering indicatrix which enteres with the radiation transfer equation by means of Legendre polynomials.

Invariant Imbedding Method [186–190]

The invariant imbedding method starts from a critique of the solution of the RTE by means of expansions of the phase function and linearization of the equations. If the scattering is highly anisotropic – as in the case of large aerosols – the linearized algebraic systems are ill-conditioned and give instable or only slowly convergent solutions. In the invariant imbedding method the integro-differential equations for the transmission and reflection functions are directly treated. The integrals are approximated by sums via Gaussian quadrature. The resulting ordinary differential equations are then integrated numerically.

Dodecaton Approach to Radiative Transfer (DART) [191]

In this method space is subdivided into a certain number (which can be arbitrarily large) of radiation streams arranged on a regular dodecahedron. The minimum number of discrete streams which has to be considered for a pre-set accuracy can be determined from Bayes' Rule of probability theory.

Approximative Similarity Solution [192]

The radiation transfer in a anisotropic scattering medium is treated as an isotropic scattering problem in which the single scattering albedo and the optical depth are adjusted by means of an asymmetry factor.

Eddington Approximation [193, 194]

In the Eddington approximation the field of scattered radiation is approximated by an isotropic distribution of the radiance which depends on the optical depth of the atmosphere and the solar zenith angle only. The phase function is approximated by $p(\vartheta) = 1 + \beta_1 \cos\vartheta$, where β_1 is constant.

Schuster-Schwarzschild Approximation [195–199]

In this approximation the incident flux is represented by a parallel beam which is broken up due to scattering in one component parallel with the incident direction and one in the opposite direction. The phase function is thus represented by a Delta-function.

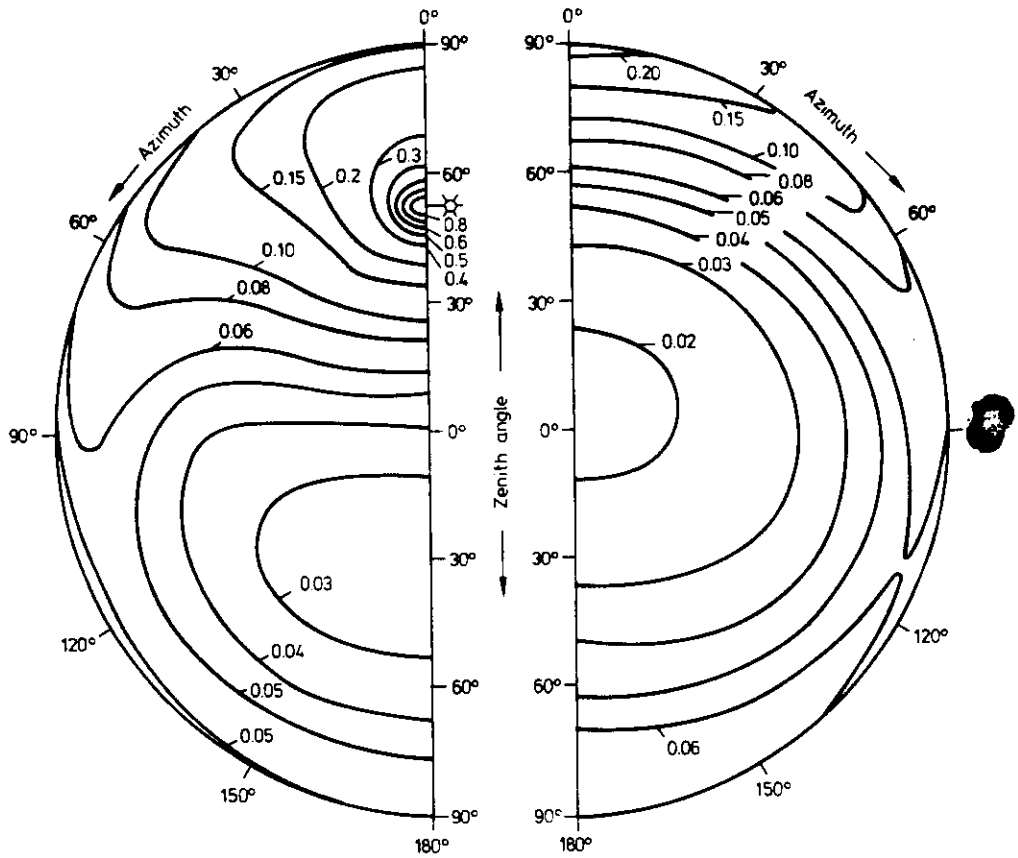

Fig. 23. Distribution of downwelling (left) and upwelling scattered solar radiance in a turbid atmosphere computed by Bakan and Quenzel [204]

Exponential Kernel Approximation [200, 201]
The phase function is approximated by a Delta-function and two Legendre terms. The exponential integrals appearing in the formal solution of the equation of radiative transfer are approximated by exponential functions in which a diffusity factor of 3/2 appears in the exponent.

Pertubation Method [202–204]
In this method only variations of the single scattering albedo with optical depth are considered. On a reference homogeneous atmosphere of constant single albedo a variable perturbation is superimposed and the deviation from the reference case is computed.

These more elaborate computations of the radiance field in scattering atmospheres result in distribution for the cloud-free atmosphere like the example reproduced in Fig. 23. There are hardly any direct comparisons between computed and measured radiances because the simultanous determination of all necessary atmospheric parameters and of the spectral radiances is difficult to accomplish. As far as comparisons could be made the computed radiances compare favourably with the features measured from the ground.

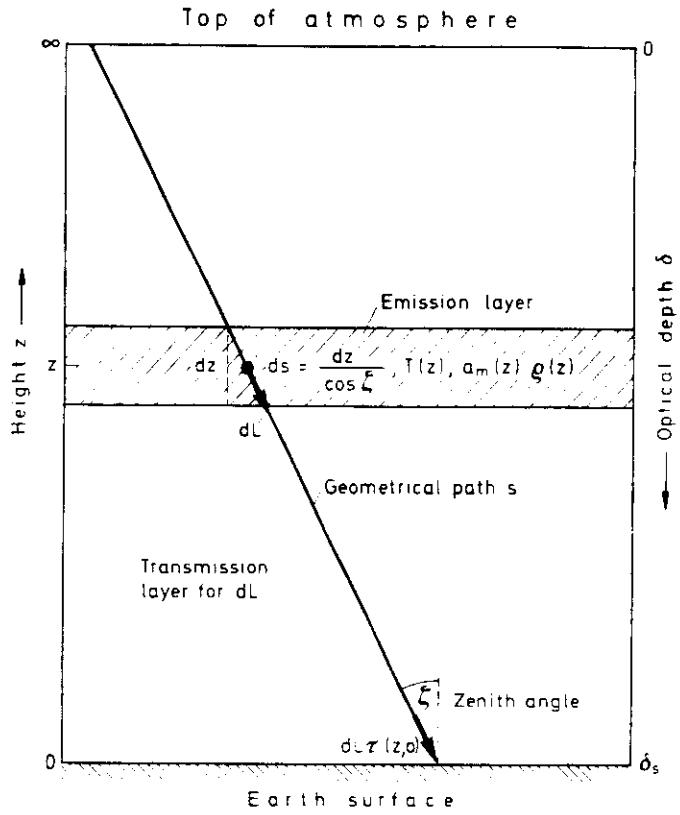

Fig. 24. Derivation of the equation of radiative transfer for an emitting atmosphere

Radiative Transfer Equation for the Terrestrial Emission

A computation of the radiance distribution has to start from Eq. (132) which defines the source function. If an inclined path is taken in a plane parallel atmosphere (Fig. 24) the contribution of an atmospheric layer of the geometrical thickness dz in the direction ζ is

$$dL = a_m \varrho(z)\, B[T(z)] \frac{dz}{\mu} \tag{137}$$

where a_m is the mass absorption coefficient and $\varrho(z)$ the density of the emitting gas. Only the fraction

$$(dL)_{z=0} = (dL)_z \tau(\mu; z, 0) = a_m(z)\, \varrho(z)\, B[T(z)] \exp\left\{-\int_0^z a_m \varrho(z) \frac{dz}{\mu}\right\} \frac{dz}{\mu} \tag{138}$$

arrives at the surface $z=0$ because of absorption between $z=0$ and z. With the optical depth between z and $z=0$,

$$\delta(z, 0) = \int_0^z a_m \varrho(z) dz, \tag{139}$$

the transmittance is $\tau(0, z) = \exp\{-\delta(z, 0)/\mu\}$.
Equation (138) can then be transformed to

$$-(dL)_{z=0} = B[T(z)] \frac{d\tau(\mu; z, 0)}{dz} \tag{140}$$

and the emission of the whole atmosphere becomes

$$L(\mu, z=0) = -\int_0^\infty B[T(z)] \frac{\mathrm{d}\tau(\mu; z, 0)}{\mathrm{d}z} \mathrm{d}z. \tag{141}$$

A more general RTE can be derived from Eq. (133) in which the source function J has to be replaced by $B[T(z)]$ defined in Eq. (88):

$$\mu \frac{\mathrm{d}L_{\bar{\nu}}(\delta, \mu)}{\mathrm{d}\delta} = L_{\bar{\nu}}(\delta) - B_{\bar{\nu}}[T(\delta)]. \tag{142}$$

Here the spectral index $\bar{\nu}$ has been added. To compute the irradiance, Eq. (142) has to be solved for $L_{\bar{\nu}}(\delta, \mu)$ and to be integrated over all directions μ. A formal solution [see Eq. (39)] is

$$E_{\bar{\nu}} = \int_{2\pi\Omega_0} L_{\bar{\nu}} \mathrm{d}\Omega = \pi \int B_{\bar{\nu}}[T(\delta_{\bar{\nu}})] \, \mathrm{d}\{2\mathrm{Ei}_3(\delta_{\bar{\nu}})\}, \tag{143}$$

where Ei_3 is the third exponential integral

$$\mathrm{Ei}_3(u) = \int_1^\infty \mathrm{e}^{-ux} x^{-3} \mathrm{d}x$$

which can be approximated by a simple exponential function ($\frac{1}{2}\mathrm{e}^{-ru}$) with a r-times elongated optical depth u. The irradiance can therefore be approximated by

$$E_{\bar{\nu}} \cong \pi \int B_{\bar{\nu}}[T(\delta_{\bar{\nu}})] \, \mathrm{d}\tau_{\bar{\nu}}(\mathrm{r} \cdot \delta). \tag{144}$$

r is called diffusity factor and has a mean value of 1.66.

Parameterization of the Atmospheric Band Structures

To determine the total irradiance Eq. (144) has to be integrated over all wavelengths. The difficulty to solve the RTE (144) lies in the determination of the transmission functions. Several gases with highly variable absorption coefficients and partly overlapping bands contribute to the radiation flux. Different approaches are in use to deal with this problem.

a) *Computation from Basic Line Parameters* [84, 205, 206]

The atmosphere is subdivided in a number of levels with constant temperature and density of the absorbing molecular species (H_2O, CO_2, O_3, CH_4, N_2O). For each wavenumber the transmission from each level to the observer (e.g. ground or space) is computed by setting a equal to the sum of all individual line contributions [Eq. (77)]. In the 8–13 μm window region also the water vapor continuum and the aerosol contribution has to be added as described earlier.
The radiance is then computed by replacing the integral by a sum over the atmospheric layers:

$$L_{\bar{\nu}} = \sum_{i=1}^{N} B_{\bar{\nu}, i}[T_i] \, \Delta_i \tau. \tag{145}$$

where

$$\Delta_i \tau = \tau(z_i, 0) - \tau(z_{i-1}, 0).$$

In order to reproduce a spectrum with high accuracy the computations have to be done in steps of $10^{-3} - 10^{-4}\,\mathrm{cm}^{-1}$ in the vicinity of line centers. The atmosphere has normally to be subdivided into 30–100 layers. One example of a computation is given in Fig. 7 [84].

b) *Computation from Averaged Empirical Band Transmissivities*

The spectrum is subdivided according to the contributions of the major molecular bands and the slope of the Planck function. For each spectral band empirical transmission functions or averaged transmission functions computed from basic line parameters and averaged Planck functions are used. Transmission functions have been measured for specific temperatures and a range of pressures [45–49]. In order to account for the temperature and pressure dependence of the transmission often standard transmission functions are used but the masses are scaled by $(p/p_0)(T_0/T)^n$ [207]. The computations then follow the procedure of equation (145) with all quantities averaged over the spectral

intervals. Finally the partial spectrally averaged radiances are summed up to compose the total radiance.

It is also possible to average first the transmittance spectrally for all absorbers and to solve Eq. (145) only once. This can then be done graphically by means of radiation diagrams [208–210].

c) *Emissivity Method* [211, 212]

The RTE can be re-formulated by introducing the emissivity instead of the transmission. The emissivity ε at pressure p and temperature T for the mass m for the whole spectrum is defined by

$$\varepsilon(m, p, T) = \frac{1}{\sigma T^4} \int_0^\infty a_\nu(m, p, T)\, B_\nu(T)\, \mathrm{d}\nu. \tag{146}$$

With $1 - \tau = \varepsilon$ the irradiance can thus be written

$$E = \int_z^\infty B_\nu(z') \left(\frac{\mathrm{d}\varepsilon_\nu(z, z')}{\mathrm{d}z} \right) \mathrm{d}z'$$

$$\varepsilon_\nu(z, z') = \int_z^\infty \int_0^\infty \frac{\pi B_\nu(z'')}{\sigma T^4(z'')} \frac{\mathrm{d}a_\nu}{\mathrm{d}z''} \,\mathrm{d}\nu\, \mathrm{d}z''. \tag{147}$$

The integrals over the wavenumber can be computed in advance so that for the direct application only the integration over the atmosphere remains to be solved.

General Energy Budget Equations for an Earth-Atmosphere System

The global energetics develop from an interplay of the processes which occur on regional scales in areas of varying boundary conditions. It seems appropriate therefore to start the discussion with a description of the energy processes in a cell or a "cage" which extends from the ocean or solid earth to the top of the atmosphere. The cage will extend into the ocean or solid earth as far as it is affected by energy transports. For the oceans this depth is difficult to assess since climate variations may affect the deep ocean but only after a long time period. The exchange between the deep ocean and its upper layers is in the order of several hundred years. If we restrict ourselves to shorter time periods the deep ocean will be decoupled from the system and we need only to be concerned about the upper layers of the ocean, the "warm water sphere" or the top layer of the ocean with a few hundred meters thickness (compare Fig. 1).

If the flux divergencies in such a cage or box can be determined from its physical properties and chemical composition then it will later on be possible to connect all these boxes in order to construct a global system [213, 214].

To establish the energy budget of the volume all energy fluxes into and out of such an elementary box of the earth-atmosphere system have to be considered (Fig. 25). The *external input* is the solar energy flux which may be partly compensated or in other locations overcompensated by the infrared emission to space. It is possible that at the surface some of the solar energy is stored for some time, generally half a year, if the system is in a steady state. This implies that there is no accumulation or loss of energy over periods of one or more years.

There are other energy transfers through the vertical walls of the volume, transports which are accomplished by the general circulation of the atmosphere and the oceans. These fluxes are called *advective fluxes*. It is assumed that horizontal radiative transports are neglegible and that only heat as well as potential and

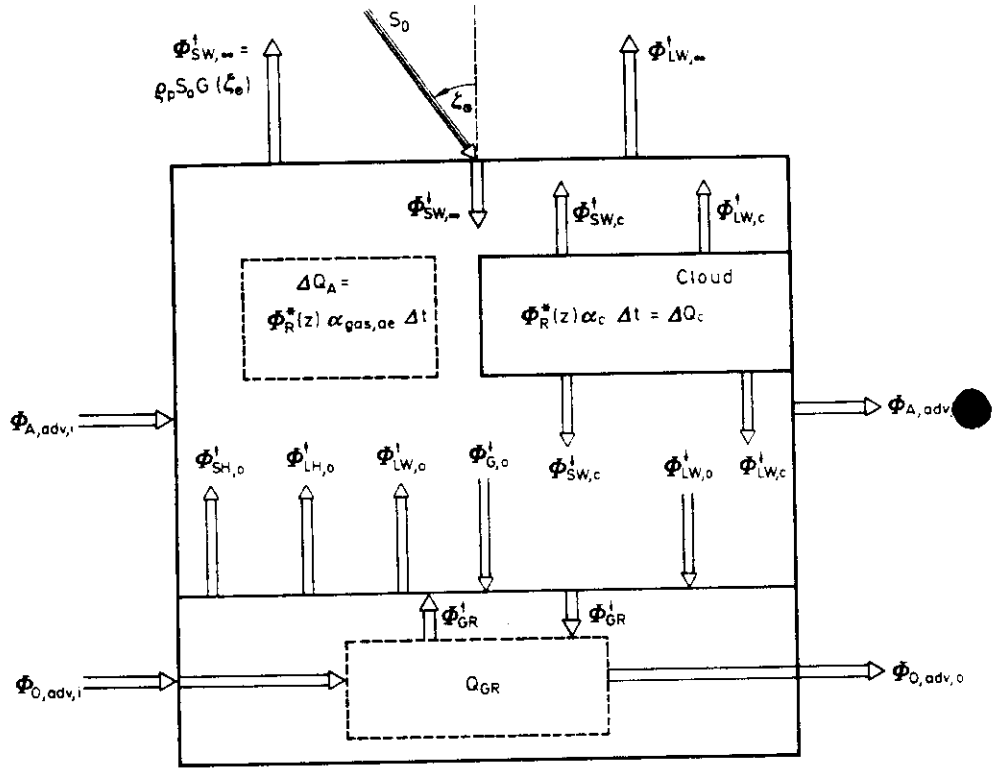

Fig. 25. Energy fluxes within and across the boundaries of an ocean-atmosphere volume

kinetic energies are transported this way. These transports compensate for any gain or loss of radiant energy within the box over longer time scales. Excess energy of one volume is horizontally transported to areas with energy deficits. The mechanism set into action to maintain these transports is the general circulation of the atmosphere and the oceans.

Within an elementary volume energy conversions as discussed in the introduction take place. At the surface energy arriving as solar radiation is transformed to conductive heat fluxes into the surface and the atmosphere. A substantial part of the energy is used to evaporate water which is transported as latent energy into the atmosphere. The heat flow into the atmosphere at the ground generates buyancy which carries heat upward by turbulent processes. Latent heat can be released if condensation occurs and clouds are building up. The heat released during condensation warms the atmosphere further and potential energy builds up by the rising air masses, generating pressure gradients which eventually require an outflow of these elevated masses across the walls of the volume, compensated by an inflow at lower levels. Thus potential energy disappears and kinetic energy is generated, which finally is destroyed by friction at the surface and inbetween the air molecules.

In order to quantify the relations between the different fluxes of energy in the earth-atmosphere system fundamental mathematical relations are sought now. The imaginated volume extends a few hundred meters into the oceans or a few meters into the soil, as far as the annual winter-to-summer temperature variations reach. In Fig. 25 only an ocean is considered for the lower boundary of the atmosphere. In the case of solid earth there would be no horizontal fluxes through this part of the volume but the picture would essentially remain the same.

At the top of the atmosphere the solar irradiance S_0 is incident under a zenith angle $\zeta_\odot$. It generates a flux $\Phi^{\downarrow}_{SW,\infty} = S_0 A G(\zeta_\odot)$ into the volume. $G(\zeta_\odot)$ is a geometry factor which would be identical to $\cos\zeta_\odot$ for a plane parallel atmosphere and deviates from this function slowly if $\zeta_\odot > 75°$. A is the horizontal area of the atmosphere-surface system. Part of the shortwave radiation is reflected and scattered back into space. This fraction is $\varrho_p \Phi^{\downarrow}_{SW,\infty}$ where

$$\varrho_p = \Phi^{\uparrow}_{SW,\infty} / \Phi^{\downarrow}_{SW,\infty} \tag{148}$$

is the *planetary albedo*.

The atmosphere-earth-surface system will also emit infrared radiation, $\Phi^{\uparrow}_{LW,\infty}$, to space. The radiation budget at the top of the atmosphere is therefore

$$\Phi^{*}_{R,\infty} = \Phi^{\downarrow}_{SW,\infty}(1-\varrho_p) - \Phi^{\uparrow}_{LW,\infty}. \tag{149}$$

The budget is positive if energy is provided to the system. The star is used for the difference of the fluxes with opposite direction through a surface and is referred to as *net flux*.

At the surface a fraction of $\Phi^{\downarrow}_{SW,\infty}$ arrives partly as direct $[\Phi^{\downarrow}_{SW,\infty}\tau(0,\infty)]$ and partly as scattered or diffuse solar radiation $\Phi^{\downarrow}_{d,0}$. The sum of these two components is called *global radiation* $\Phi^{\downarrow}_{g,0}$:

$$\Phi^{\downarrow}_{g,0} = S_0 A G(\zeta_\odot)\tau(0,\infty) + \Phi^{\downarrow}_{d,0}. \tag{150}$$

The *radiation budget* at the *surface* consists of four components, the downwelling shortwave and longwave fluxes, the reflected shortwave flux and the flux of the emitted longwave radiation:

$$\Phi^{*}_{R,0} = \Phi^{\downarrow}_{g,0}(1-\varrho_0) + \Phi^{\downarrow}_{LW,0} - \Phi^{\uparrow}_{LW,0}. \tag{151}$$

ϱ_0 is the surface albedo.

From the surface the fluxes of sensible and latent heat are directed into the atmosphere, and another heat flux into the ground, the ocean or the soil. In these media the energy may be stored or transported away. The energy budget of the ground volume is therefore

$$\Phi^{*}_{R,0} + \Delta\Phi_{0,adv} - \Phi^{*}_{SH,0} - \Phi^{*}_{LH,0} - \Phi_{PH} = \frac{\partial Q_{GR}}{\partial t} = \frac{1}{\varrho c}\frac{\partial T_{GR}}{\partial t}. \tag{152}$$

$\Delta\Phi_{0,adv} = \Phi_{0,adv,i} - \Phi_{0,adv,o}$, influx minus outflux through ocean, and Φ_{PH} is the flux which is used for photosynthesis and which is therefore stored in biological mass (less than 1% of $\Phi^{\downarrow}_{SW,0}$). That part of the net flux which is stored in the ground, $\Phi^{\downarrow}_{GR,0}$, raises the temperature of the surface layer of the ground and thus affects the emitted longwave radiation which will be raised according to the

surface temperature until the opposite process starts. The heating respectively cooling which occurs is expressed by the r.h.s. of Eq. (152).

The budget of the atmosphere is in analogy to Eq. (152):

$$\Phi^*_{R,\infty} - \Phi^*_{R,0} + \Phi^*_H + \Delta\Phi_{A,adv} = \frac{\partial Q_A}{\partial t} = \frac{1}{\varrho c_p}\frac{\partial T_A}{\partial t}. \tag{153}$$

Here the latent and the sensible heat fluxes are combined to Φ_H and the star is used in order to indicate that there are also reversed fluxes due to dew and precipitation.

Combination of Eqs. (152) and (153) results in

$$\frac{\partial Q}{\partial t} = \Phi^*_{R,\infty} + \Delta\Phi_{adv} - \Phi_{PH}, \tag{154}$$

where $\partial Q/\partial t$ is the rate of storage in the whole system.

If Φ_{PH} is neglected in Eq. (154) and if the fluxes are averaged over a year or a number of years one can assume that $\partial Q/\partial t = 0$ (if there are no climate changes), and therefore

$$\bar{\Phi}^*_{R,\infty} = \overline{\Delta\Phi}_{adv}. \tag{155}$$

Averaged over a period of one year (or several years) the radiation budget at the top of the atmosphere equals the divergence of energy advected into the volume by both, the oceans and the atmosphere.

If Eq. (155) is furthermore zonally averaged it is clear that there can be no flux across the poles and Eq. (155) can be rewritten in the following way. The earth is subdivided into N latidudinal zones i, defined by corresponding geographical latitudes φ_i.

$$[\overline{\Delta\Phi}_{adv}]_i = [\bar{\Phi}_{adv}(\varphi_i)] - [\bar{\Phi}_{adv}(\varphi_{i-1})]. \tag{156}$$

Applied to Eq. (155) it results

$$\sum_{i=1}^{N} [\bar{\Phi}^*_{R,\infty}]_i = \sum_{i=1}^{N} [\overline{\Delta\Phi}_{adv}]_i = \bar{\Phi}_{adv}(\varphi_N) - \bar{\Phi}_{adv}(\varphi_o). \tag{157}$$

If the summation starts at one pole ($\varphi_o = 90°$) where $\bar{\Phi}_{adv}(\varphi_o) \equiv 0$, then the sum of N zonal mean net radiation fluxes at the top of the atmosphere represents the advective flux across the latitude φ_N.

The zonally averaged advective fluxes in the earth-atmosphere system can therefore be determined by careful measurements of the zonal radiation budgets from space. This quantity is a boundary condition for the processes in the system but does not yet provide much insight into the processes within the system itself, especially because it is not yet possible to discriminate between oceanic and atmospheric transports and to define those transports which finally determine the environmental or internal system conditions.

From satellite observations and computations using conventional data [215–219] it can be concluded that the total transport is in the order of the numbers given in Table 20.

In order to gain more insight into the functioning of the system the next step is to inspect more closely what happens at the borders of the box volume and

Table 20. Zonally averaged radiation budget parameters and meridional fluxes. (After Ellis and Van der Haar [238] but balanced with respect to total energy budget)

Latitude zone in degree	Area $4\pi R^2$ in %	Area in $10^{12}\,m^2\,(10^\circ)^{-1}$	Length of zonal circle in 10^6 m	Annual mean solar irradiance in $W\,m^{-2}$	Balanced zonal net energy input in $PJ\,(10^\circ)^{-1}\,s^{-1}$	Horizontal flux across latitude in PW	Horizontal flux per unit latitude in $GW\,m^{-1}$	
80–90 N	0.760	3.88	6.948	173.9	−0.405	+0.405	+0.058	↑ Northward
70–80	2.255	11.50	13.688	185.5	−1.087	+1.492	+0.109	
60–70	3.685	18.79	20.012	213.5	−1.373	+2.865	+0.143	
50–60	5.000	25.49	25.727	260.5	−1.214	+4.079	+0.159	
40–50	6.160	31.41	30.658	307.0	−0.686	+4.765	+0.155	
30–40	7.140	36.41	34.661	347.7	−0.008	+4.773	+0.138	
20–30	7.900	40.28	37.610	380.1	+0.696	+4.077	+0.108	
10–20	8.420	42.93	39.415	402.4	+1.914	+2.163	+0.055	
0–10	8.680	44.26	40.024	414.1	+2.566	−0.403	−0.010	
0–10 S	8.680	44.26	39.415	414.1	+2.442	−2.845	−0.072	
10–20	8.420	42.93	37.610	402.4	+1.708	−4.553	−0.121	
20–30	7.900	40.28	34.661	380.1	+0.849	−5.402	−0.156	
30–40	7.140	36.41	30.658	347.7	−0.016	−5.386	−0.176	
40–50	6.160	31.41	25.727	307.0	−0.887	−4.499	−0.175	
50–60	5.000	25.49	20.012	260.5	−1.487	−3.012	−0.151	
60–70	3.685	18.79	13.688	213.5	−1.626	−1.386	−0.101	
70–80	2.255	11.50	6.948	185.5	−1.041	−0.345	−0.050	↓ Southward
80–90	0.760	3.88		173.9	−0.345			
Total	100.0	$0.5099 \cdot 10^{15}\,m^2$			0.0			

what transformations occur within the volume. We start with this discussion at the top of the atmosphere.

Energy Fluxes at the Top of the Atmosphere

Solar Irradiance

The upper boundary of the atmosphere is distinguished by the fact, that energy transfer occurs only by radiation, of which the solar radiation is the single incident component. Its normal incidence flux area-density, the solar constant S_0, has been determined from high altitude observatories by extrapolation of spectral measurements to zero air mass [61, 62], as well as from aircraft [63, 220], Balloons [65, 221–224], rockets [225] and more recently also from satellites [226–229]. The conclusions drawn from two different subsets of the data presented in Fig. 26 differ considerably. Vonder Haar et al. [230] and Fröhlich [231] arrive at an unweighted mean of $1{,}377 \pm 20\ \mathrm{W\,m^{-2}}$ with a standard deviation of $8\ \mathrm{W\,m^{-2}}$. Brusa and Fröhlich [232a] and Crommelynck [232b] give a value of $1{,}367 \pm 5\ \mathrm{W\,m^{-2}}$. The higher values are not in accordance with other radiation budget studies [229], where a value of $1{,}368\ \mathrm{W\,m^{-2}}$ would be preferable. A conservative figure for the solar constant would therefore presently be

$$S_0 = 1{,}370 \pm 8\ \mathrm{W\,m^{-2}}. \tag{158}$$

The solar constant was believed to be about $9\ \mathrm{W\,m^{-2}}$ lower than this value more then a decade ago and rose to more than $1{,}370\ \mathrm{W\,m^{-2}}$ in the early 1970ies. but these discrepancies can be explained by the improving but still not perfect measuring techniques. There is therefore no indication of a real trend in this fundamental quantity [232c]. Only Kondratyev and Nikolsky [222] reported unconfirmed changes of S_0 in the order of 2.5% over a period of five years. Strong

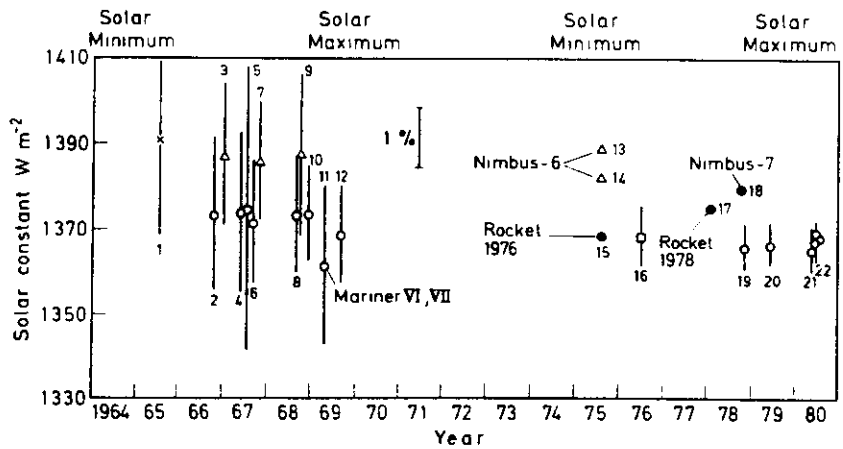

Fig. 26. Experimental determinations of the solar constant during the last decennia. (After Fröhlich [231], Vonder Haar et al. [230], and Brusa and Fröhlich [232])

variations which increase in amplitude with decreasing wavelengths below 200 nm are observed in the uv part of the solar spectrum [233]. Brusa et al. has recently also reported [232a] short term fluctuation with periods between 5 and 20 min of the solar flux. The amplitude of these short-term fluctuations are in the order of 0.1‰, again growing with decreasing wavelength. Willson et al. [232d] detected variations of the total solar irradiance from the Solar Maximum Mission spacecraft around the mean value of 1,368.31 $W\,m^{-2}$ in the order of $\pm 0.05\%$. Such fluctuations occur in the frequency range below 0.15 day^{-1}. Two larger decreases in irradiance of up to 0.15%, each lasting for about one week, have also been observed. These two decreases are apparently correlated with the development of large sunspot groups.

A new attempt to measure the solar constant will be made from future space missions. By means of the carefully designed instruments which are nowadays available, it should be possible, to measure the long term variability of the solar constant to 0.1% or 1.4 $W\,m^{-2}$ precision, and to correlate measured variations with the solar rotation or solar activity. The absolute mean value stated in Eq. (158) may in the future still be object to corrections by a few $W\,m^{-2}$.

The knowledge of the solar constant is of fundamental importance for the determination of the equilibrium state of the earth. Variations of the mean solar input will immediately induce climate variations.

The geographical distribution of the solar irradiance at the top of the atmosphere is determined by astronomical parameters like the earth orbit around the sun and the inclination of the earth rotation axis with respect to the plane of the earth orbit, the ecliptic.

The earth orbit is an ellipse with a ratio minor axis to major axis of 0.967. The mean distance between sun and earth (= semimajor axis of orbit) is called 1 Astronomical Unit (A.U.) for which the internationally accepted value is $149.5 \cdot 10^6$ km. The earth presently is at its mean distance from the sun on April 3 and October 5. The minimum distance ($147.1 \cdot 10^6$ km), the perihelion, is passed on January 5 and the maximum distance ($152.1 \cdot 10^6$ km) the aphelion, on July 5.

The rotation axis of the earth is tilted against the orbital plane by 23°27'08".2 at the present time. Thus the sun is in the equatorial plane of the earth only twice a year, on March 21 and September 23, at equinox. The north pole is tilted against the sun on December 21 and the south pole on June 21. These positions are called solstices. The angle between the equatorial plane and the sun is the declination $\delta_\odot$ which accordingly varies during the year between about +23°5 (June 21) and −23°5 (December 21).

The irradiance at the position of the earth depends on the distance between sun and earth. The geographical distribution of the irradiance on top of the atmosphere is a function of the solar zenith angle $\zeta_\odot$ which can be expressed by the geographical latitude φ, the declination $\delta_\odot$, and the time between local noon and the hour of observation. Since one rotation of the earth around its axis takes 24 h for 360°, the angle of rotation corresponding to one hour is 15°. Therefore

$$h = (15 \cdot \Delta t_\odot)^\circ, \tag{159}$$

where h is the angle of rotation corresponding to the difference $\Delta t_\odot$ between the true local time (TLT) t and true local noon in hours:

$$\Delta t_\odot = t - 12.00 \quad \text{(true local time)}. \tag{160}$$

$\Delta t_\odot$ is negative in the morning, positive in the afternoon. The True Local Time (TLT) is related to the Local Mean Time (LMT) by the equation of time, Δt, which is normally presented in tabular form (72):

$$\Delta t = \text{TLT} - \text{LMT}. \tag{161}$$

This difference arises because the rotation of the earth is not constant during the year. The variation has the magnitude of −14.33 min (12. Feb.) to +16.4 min (3. Nov.) with two secondary peaks (+3.73 min on 13. May and −6.42 min on 27. July). Clocks are measuring Zone Mean Times (ZMT) which generally change by one hour every 15° longitude starting at Greenwich (0°). This has to be taken into account if one transfers ZMT to TLT:

$$t(\mathrm{TLT}) = (\lambda - \lambda_R) \cdot \tfrac{1}{15} + t(\mathrm{ZMT}) + \Delta t\,, \tag{162}$$

where
λ_R = ZMT reference longitude
λ = longitude of observation site in degree (positive to east).
From spherical geometry the following equation for the solar zenith angle can be derived if the reference plane is tangential to the earth surface:

$$\cos\zeta_\odot = \sin\varphi \sin\delta_\odot + \cos\varphi \cos\delta_\odot \cos h\,. \tag{163}$$

The irradiance at the top of the atmosphere is

$$S = S_0 \left(\frac{\bar{d}}{d}\right)^2 \cos\zeta_\odot\,. \tag{164}$$

S_0 is the irradiance at $\bar{d} = 1$ A.U., and d the actual distance between earth and sun.

The integration of Eq. (164) over the day gives the radiant exposure measured in $\mathrm{Ws\,m^{-2}}$ or $\mathrm{Jm^{-2}}$ per 24 h:

$$H(\varphi, \delta_\odot) = \frac{8.64 \cdot 10^4}{\pi} S_0 \left(\frac{\bar{d}}{d}\right)^2 [h \sin\varphi \sin\delta_\odot + \cos\varphi \cos\delta_\odot \sin h]\,. \tag{165}$$

$8.64 \cdot 10^4$ are the seconds per day and h is the length of the half day, e.g. from sunrise to noon in radian and is defined by Eq. (163) with $\zeta_\odot = 0$:

$$\cos h = -\operatorname{tg}\varphi \operatorname{tg}\delta_\odot\,. \tag{166}$$

For locations and times where the sun does not set it is $h = \pi$ and

$$H(\varphi, \delta_\odot) = 8.64 \cdot 10^4 S_0 \left(\frac{\bar{d}}{d}\right)^2 \sin\varphi \sin\delta_\odot\,. \tag{167}$$

For $\delta_\odot = +23.5°$ this happens to be for

$$\operatorname{tg}\varphi = \frac{1}{\operatorname{tg} 23.5} = 2.3\,, \quad \text{or} \quad \varphi = 66.5\,\mathrm{N}\,.$$

As an example the equator at equinox ($\delta_\odot = 0$, $\varphi = 0$, $\bar{d}/d \cong 1$) receive $37.6 \cdot \mathrm{MJ\,m^{-2}}$ per day. At solstice the (north) summer pole ($\delta_\odot = 23.5$, $\varphi = 90°$, $\bar{d}/d = 0.967$) receives by the factor $(\bar{d}/d)^2\, h \sin 23.5 = 0.967^2 \cdot \pi \cdot \sin 23.5 = 1.17$ more energy than the equator at equinox; and the equator ($\varphi = 0$) receives at solstice $0.967^2 \cos 23.5 = 0.857$ times the energy incident at the equator at the time of the equinox.

Planetary Albedo

A fraction of the solar radiation is scattered or reflected back to space. The ratio of the outgoing shortwave flux density M to the incoming solar irradiance S is the instanteaneous planetary albedo ϱ_p of the earth at the geographical coordinates φ and λ:

$$\varrho_p(\varphi, \lambda) = M^{\uparrow}_{SW,\infty}(\varphi, \lambda)/S(\zeta_\odot)\,, \tag{168}$$

where $S(\zeta_\odot)$ is given by Eq. (164).

The planetary albedo in a certain area is a function of the cloudiness and the albedo of the clouds, the turbidity of the atmosphere, the scattering characteristics of the aerosol, and of the surface albedo. It is quite difficult to compute the

planetary albedo since multiple scattering processes in the atmosphere-surface system have to be taken into account. If one disregards this complexity, one may approximately write

$$\varrho_p \cong N_h \varrho_{c,h} + N_m \varrho_{c,m} + N_l \varrho_{c,l} + (1-N)\{\tau^2(0,\infty)\varrho_s + \varrho_a\}. \quad (169)$$

Here

N_h, N_m, N_l	are the fractions of coverage for high, medium and low cloud tops in the measured area
$\varrho_{c,h}, \varrho_{c,m}, \varrho_{c,l}$	the albedos of the high, medium and low clouds respectively
ϱ_s	surface albedo
ϱ_a	the albedo of the cloudless atmosphere due to molecule and aerosol scattering
$N = N_h + N_m + N_l$	total cloudiness
$\tau(0, \infty)$	transmission of the cloudfree atmosphere from the ground to space

In Eq. (169) the first three terms on the r.h.s. include the albedo of the atmospheric gases on top of the clouds.

The albedo produced by the scattering atmosphere, ϱ_a, depends on the concentration of aerosols in the atmosphere and its scattering characteristics. The molecular component of the atmosphere produces an average albedo of approximately 8% depending on the mean solar zenith angle (Table 21) which has a maximum value of 39.5° at equinox for the equator. Values of the planetary albedo are compiled in Table 20 after computations made by Braslau and Dave [234, 235]. If the effect of molecules, aerosol, water vapor, ozone, carbon dioxide and oxygen is considered, the average backscatter of the cloudless atmosphere is about 10%, a value which is also observed over the oceans outside the solar reflex [236].

The albedo of clouds depends on the type of cloud, water cloud or ice cloud, and the thickness or liquid water respectively ice content of the cloud. There have been several attempts to determine the average planetary albedo of a cloudy sky and its geographical distribution either by computations based upon cloud observations, local surface albedo measurements and aerosol estimates, or by direct measurements made from satellites. In Fig. 27 some of the more recent results from satellite measurements are reproduced.

The mean value of the planetary albedo which is presently the most probable one [229, 238] is

$$\varrho_p = 0.305. \quad (170)$$

The range of earlier determination was between 0.35 [218] and 0.29 [215].

Terrestrial Longwave Radiation

Infrared radiation is emitted by the earth surface, cloud tops and atmospheric gases like water vapor, carbon dioxide, ozone and, to a much lesser extent, CH_4 and nitrogen oxides. The total emission from a black surface into the hemisphere is according to the law of Stefan and Boltzmann given by

$$M_B(T) = \sigma T^4, \quad (171)$$

Table 21. Planetary albedo for a mid-latitude summer atmosphere after Braslau and Dave [234, 235]

Solar zenith angle	0°			30°			60°			80°		
Albedo of underlying surface	0.0	0.1	0.3	0.0	0.1	0.3	0.0	0.1	0.3	0.0	0.1	0.3
Rayleigh scattering	0.05	0.14	0.27	0.06	0.14	0.33	0.09	0.18	0.35	0.17	0.25	0.41
Rayleigh scattering and gas absorption	0.04	0.12	0.26	0.05	0.12	0.26	0.07	0.14	0.28	0.15	0.21	0.32
Rayleigh scattering, gas absorption and												
a) average haze L [26] aerosol scattering	0.05	0.12	0.26	0.06	0.13	0.27	0.10	0.16	0.29	0.22	0.27	0.37
b) average aerosol scattering and absorption	0.05			0.06			0.09			0.21		
Rayleigh scattering, gas absorption and												
a) heavy haze L [26] aerosol scattering (4 times increased particle concentrations in the stratosphere and in the boundary layer)	0.07	0.14	0.27	0.09	0.15	0.29	0.16	0.22	0.28	0.34	0.38	0.45
b) heavy aerosol scattering and absorption	0.06			0.08			0.14			0.31		

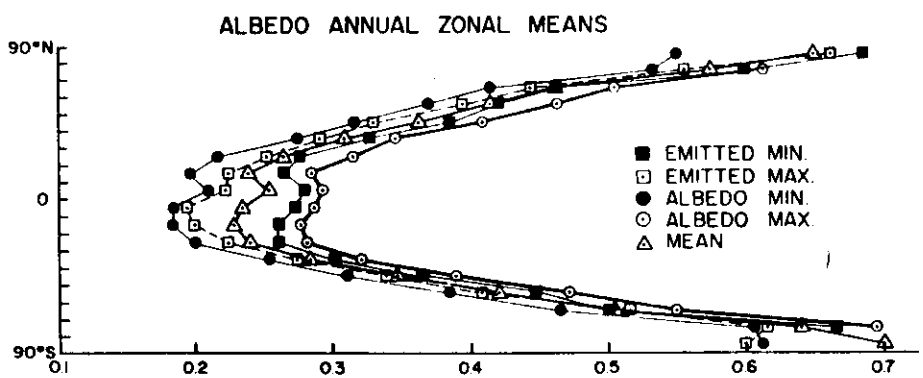

Fig. 27. Annual average and variability of zonally averaged planetary albedo distribution with latitude. (After Campbell and Vonder Haar [237])

where

$$\sigma = 5.6696 \cdot 10^{-8}\ \mathrm{W\,m^{-2}\,K^{-4}}$$

is the Stefan-Boltzmann constant, and T the temperature in degree Kelvin. The relation (171) results from an integration of Eq. (86) over all wavelengths.

The maximum of the emission for terrestrial temperatures per unit wavelength interval is around 10 μm (for unit wavenumber interval around 600 $\mathrm{cm^{-1}}$ or 17 μm compare Figs. 15 and 16) following from Planck's law, Eqs. (86), (87), which is graphically presented in Fig. 8. In the region between 8 and 13 μm wavelength the atmosphere is rather transparent so that a direct exchange between surface and space can take place, except for the region of the ozone band (9–10 μm). The water vapor continuum as well as aerosol absorption do, as mentioned earlier, weaken this direct radiant energy transfer. The emission of a specific area of the earth can be computed from the contributions of the different constituents of the emitting system. If again the N_i, i = l, m, or h, denote the fraction of low, medium and high cloud coverage as seen from the top of the atmosphere, and $\tau_\Phi(z, \infty)$ being the spectrally averaged transmittance for the flux between the altitude z and the top of the atmosphere, then the flux on top of area A will be with $N = \sum_i N_i$:

$$\Phi_{LW} = \varepsilon_s M_B(T_s)(1-N)\tau_\Phi(0,\infty) + \sum_{i=1}^{3} \varepsilon_i N_i M_B(T_i)\tau_\Phi(z_i,\infty) + (1-N)\int_0^\infty M_B[T(z)]\frac{d\tau_\Phi}{dz}dz + \sum_{i=1}^{3} N_i \int_{z_i}^{\infty} M_B[T_i]\frac{d\tau_\Phi}{dz}dz\,. \tag{172}$$

ε_s and ε_i are the emissivities of the surface and of the cloud tops respectively. The first r.h.s. term is the emission of the surface to space in cloud-free areas, the second term the contribution of three cloud layers, the third and forth terms the contribution of the atmosphere on top of the cloud free surface and on top of the three cloud layers respectively.

Maximum temperatures occur at the surface in deserts or semi-arid areas. The highest temperatures are about 330 K. The lowest temperature ever recorded at the surface is 184.9 K (Antarctica, 78° S, 3,420 m altitude) and minimum temperatures occur in the tropical tropopause level with 180 K (compare Fig. 1). Temperature in the earth atmosphere system vary therefore by about 255 ± 75 K or ±30%. Now the infrared emission varies with T^4 and if we take the extremes the maximum variability of local emissions can in fact be 1:10. However, since the coldest temperatures are in the tropopause in lower latitudes where at the surface the warmest temperatures occur and since at the poles the cold surface temperatures are partly compensated by a relatively warmer atmosphere, the emission at the top of the atmosphere appear much more uniform. In fact the equator to pole gradient of the infrared exitance is only 2.2 in the annual mean for the southern hemisphere (compare Fig. 28).

A computation of this quantitiy needs considerable effort since the atmospheric temperature structure, the heights and emissivities of the clouds and the cloud distribution *as seen from the top* of the atmosphere have to be known. Satellites do in fact contribute essentially to determine some of these parameters

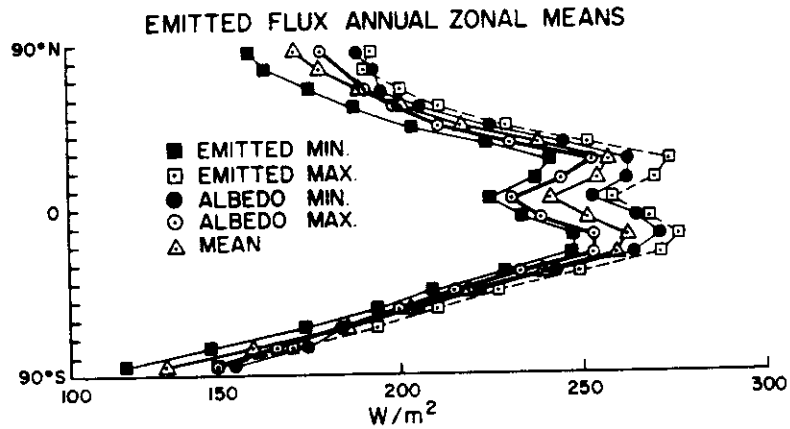

Fig. 28. Annual average and variability of zonally averaged longwave exitance of the earth-atmosphere system. (After Campbell and Vonder Haar [237])

[239, 240]. By means of special instrumentation and application of sophisticated evaluation procedures to operational meteorological satellite data the total outgoing longwave flux is also directly measured from satellites. One example of the results obtained so far is reproduced in Fig. 28.

Equilibrium Condition

For the limited time period of a few years it can be assumed that there is virtually no climate trend. Over periods of one or more full years the radiation budget at the top of the atmosphere must then be assumed to be balanced: there is no accumulation or loss of energy in the total system. Under these circumstances the absorbed solar energy must completely be re-emitted as infrared radiation. Let r_E be the radius of the planet. πr_E^2 is its cross section with respect to the parallely incident solar radiation, $4\pi r_E^2$ its surface, and ϱ_p its mean planetary albedo. The absorbed solar energy is $\pi r_E^2 S_0(1-\varrho_p)$ and the emitted infrared radiation can be set equal to $4\pi r_E^2 \sigma T_e^4$ where T_e is an equivalent emission temperature for the longwave radiation emerging from the different sources in the atmosphere: surface, clouds, aerosols and gases. The condition for radiative equilibrium is

$$\pi r_E^2 S_0(1-\varrho_p) = 4\pi r_E^2 \sigma T_e^4 . \tag{173}$$

For T_e it follows therefore:

$$T_e = \sqrt[4]{\frac{S_0(1-\varrho_p)}{4\sigma}} . \tag{174}$$

With $\varrho_p = 0.31$ and $S_0 = 1{,}370\ \mathrm{W\,m^{-2}}$ the equivalent temperature T_e becomes 254 K. For a standard mean atmosphere with a surface temperature of 288 K the temperature of 254 K occurs at about 5.2 km altitude. This level can therefore

be assumed as the average emission level, which results from the distribution of clouds and emitting gases in the atmosphere.

It can easily be seen what would happen, if either the solar constant or the albedo of the planet would change. Differentiation of Eq. (174) gives:

$$\frac{\partial T_e}{T_e} = \frac{1}{4}\frac{\partial S_0}{S_0} \tag{175}$$

respectively

$$\frac{\partial T_e}{T_e} = -\frac{1}{4}\frac{\partial \varrho}{1-\varrho}. \tag{176}$$

If the solar constant varies by 1% then the equivalent temperature changes by 0.01 $T_e/4$ or 0.64 K. In this estimate it is assumed that the albedo does not change during the transition which is not for sure. If on the other hand the solar constant remains unchanged but the planetary albedo changes by +1% absolute (which means e.g. from 31% to 32%) then the equivalent temperature decreases by 0.92 K. In both cases the climate on earth will be distorted. To what degree the change in the equivalent temperature may be reflected in the surface temperatures depends on the structure of the atmosphere and its re-adjustment to the new conditions.

Equation (173) suggests that the total infrared flux area density

$$M^{\uparrow}_{\mathrm{LW},\infty} = \sigma T_e^4 = \tfrac{1}{4} S_0 (1-\varrho_p) = \tfrac{1}{4} E^{*}_{\mathrm{SW},\infty} \tag{177}$$

is one forth of the net solar irradiance at the top of the atmosphere. The mean infrared flux density should therefore be 235.8 W m^{-2} which has not yet been verified empirically to better than about 5%. The net radiation flux as measured from satellites is presented in Fig. 29 (units: Wm^{-2}).

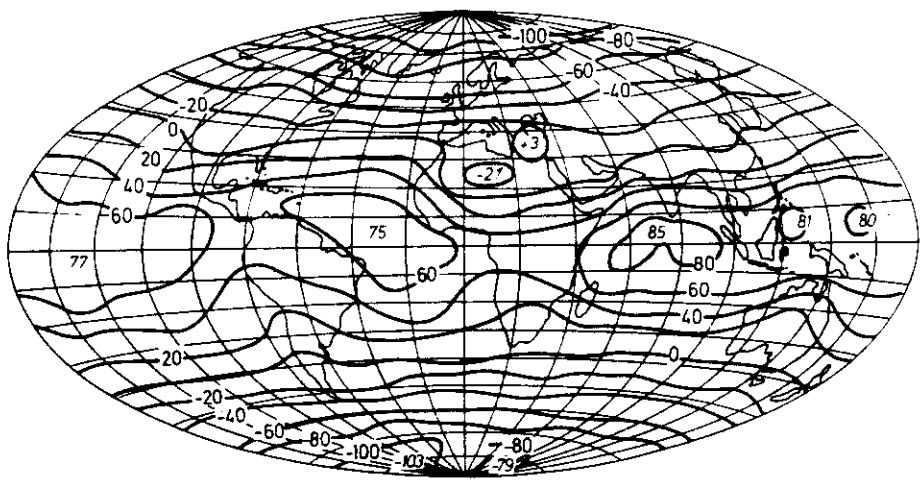

Fig. 29. Annually averaged net radiation flux area density at the top of the atmosphere. (After Vonder Haar et al. [230])